



Grain Boundary Engineering & Coincident Site Lattice (CSL) Theory

Texture, Microstructure & Anisotropy

A.D. Rollett

Last revised: 18th Mar. '14

Objectives

- The objectives of this lecture are:
- Develop an understanding of grain boundary engineering
- Explain the theory of Coincident Site Lattices (CSLs) and how it applies to grain boundaries
- Show how microstructures are analyzed for CSL content

References

- Interfaces in Crystalline Materials, Sutton & Balluffi, Oxford U.P., 1998. Very complete compendium on interfaces.
- Interfaces in Materials, J. Howe, Wiley, 1999. Useful general text at the upper undergraduate/graduate level.
- Crystal Defects and Crystalline Interfaces, W. Bollmann, (1970). New York, Springer Verlag.
- Grain Boundary Migration in Metals, G. Gottstein and L. Shvindlerman, CRC Press, 1999. The most complete review on grain boundary migration and mobility.
- Materials Interfaces: Atomic-Level Structure & Properties, D. Wolf & S. Yip, Chapman & Hall, 1992.
- Bollmann, W. (1982), Crystal lattices, interfaces, matrices. Published by the author, Geneva.
- Grimmer, H., Disorientations and coincidence rotations for cubic lattices. *Acta Crystall.* **A30** (1974) 685–688.
- Grimmer, H., Bollmann, W., Warrington, D. H., Coincidence- site lattices and complete pattern-shift lattices in cubic crystals. *Acta Cryst.* **A30** (1974) 197 – 207.
- Bonnet, R., *et al.* (1981). Determination of near-Coincident Cells Hexagonal Crystals - Related DSC Lattices. *Acta Crystall.* **A37** 184-189.
- Ikuhara, Y. and P. Pirouz (1996). Orientation relationship in large mismatched bicrystals and coincidence of reciprocal lattice points (CRLP). In: Intergranular and Interphase Boundaries in Materials, Pt 1. **207** 121-124.

Outline

- Slides from Integran with examples of Grain Boundary Engineered materials
- CSL theory
- Brandon's criterion for classification of grain boundaries by CSL type
- Technical information on comparative properties of GBE and non-GBE materials

Reading

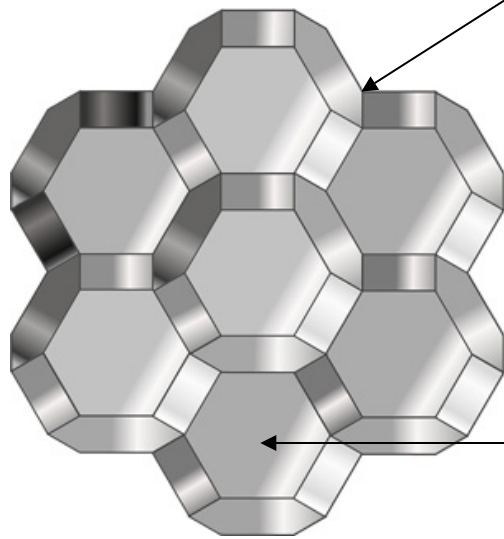
- Pages 3-25 of Sutton & Balluffi
- Pages 307-346 of Howe.

Grain Boundary Engineering

- Grain Boundary Engineering (GBE) is the practice of obtaining microstructures with a high fraction of boundaries with desirable properties.
- In general, desirable properties are associated with boundaries that have simple, low energy structures.
- Such low energy structures are, in turn, associated with CSL boundaries.
- GBE generally consists of repeated cycles of deformation and annealing, chosen so as to generate large fractions of “special boundaries” and avoid development of strong recrystallization textures.
- GBE is largely confined at present to fcc metallic systems such as stainless steel, nickel alloys, Pb, Cu.
- Note that detailed information on exactly which CSL boundaries have useful properties is lacking, as is information on how the typical processing routes actually produce high fractions of CSL boundaries.

Courtesy of:

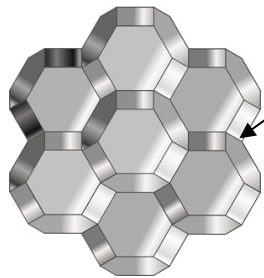
Metallurgical Nano-Technology



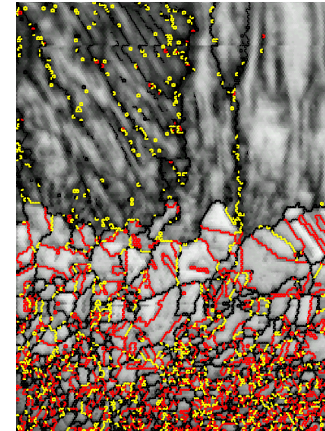
Grain boundary engineering (GBE™)

is the methodology by which the local grain boundary structure is characterized and material processing variables adjusted to create an optimized grain boundary microstructure for improved material performance.

Nanocrystalline materials are those in which the average crystal size is reduced 1000-fold from the micron-range in conventional materials to the nanometer size range (3-100nm). This can be cost-effectively achieved by proprietary electrodeposition techniques (NanoPlate™).



Grain boundary engineering (GBE™) is the methodology by which the local grain boundary structure is characterized and material processing variables adjusted to create an optimized grain boundary microstructure for improved material performance.



← Base Material
 ← GBE Surface Treatment

Boundary levels: 5.0° 15.0°
 30.00 µm = 30 steps Continuous IQ 23.7...203.6

Patent-Protected Thermo-Mechanical Metallurgical Process

Applied during component forming/fabrication processes.

Can also be applied as a surface treatment (0.1 to 1mm) to finished or semi-finished structures.

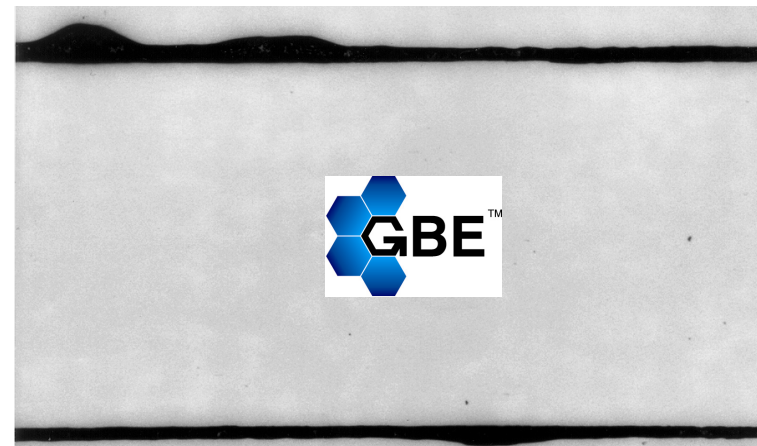
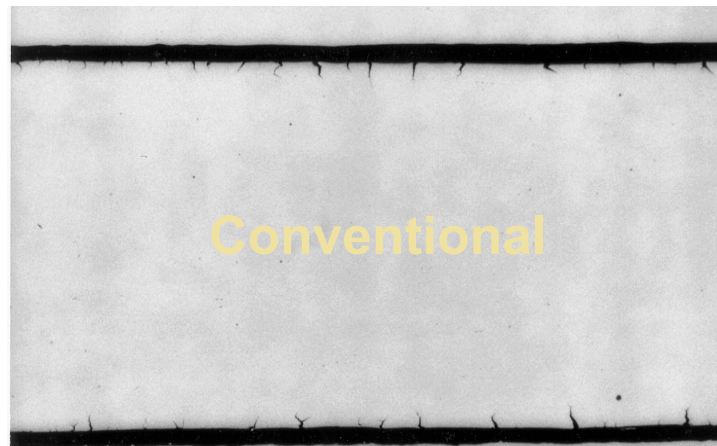
- **Increases Population of 'Special' Grain Boundaries**
- **Reduces Average Grain Size**
- **Enhances Microstructural Uniformity**
- **Fully Randomizes Crystallographic Texture**

Alloy 625

Special GB's (red; yellow)
 General GB's (black)

Integran's GBE technology has also been applied to mitigate stress corrosion cracking susceptibility of Ni-base alloys, extend the service-life of lead-acid battery grids, and improve the fatigue and creep performance of aerospace superalloys.

Alloy 690 nuclear steam generator tubing can be further optimized for SCC-resistance by GBE mill processing technology. Alloy 690 is replacing 600 in many nuclear power plants because of its enhanced resistance to SCC.



0.02 in.

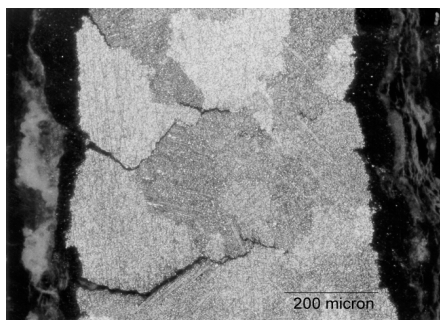
- Cross sections of sample gauge lengths following interrupted environmental CERT tests.
- Test Conditions: 60h; 10% NaOH; 600F; +0.100 mV vs. OCP; Ni Ref. Electrode; 5×10^{-7} in/sec.

See also: Alexandreanu, B., B. Capell, et al. (2001). "Combined effect of special grain boundaries and grain boundary carbides on IGSCC of Ni-16Cr-9Fe-xC alloys." *Materials Science and Engineering A* **300**(1-2): 94.

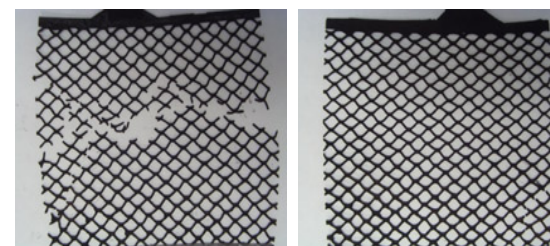
Lead-Acid Batteries

Integran's innovative GBE[®] grid processing technology is designed to extend the service life of conventional SLI and industrial batteries (US Patent No. 6,342,110 B1).

The cycle - life of lead-acid batteries (e.g., automotive) is compromised by intergranular degradation processes (corrosion, cracking).

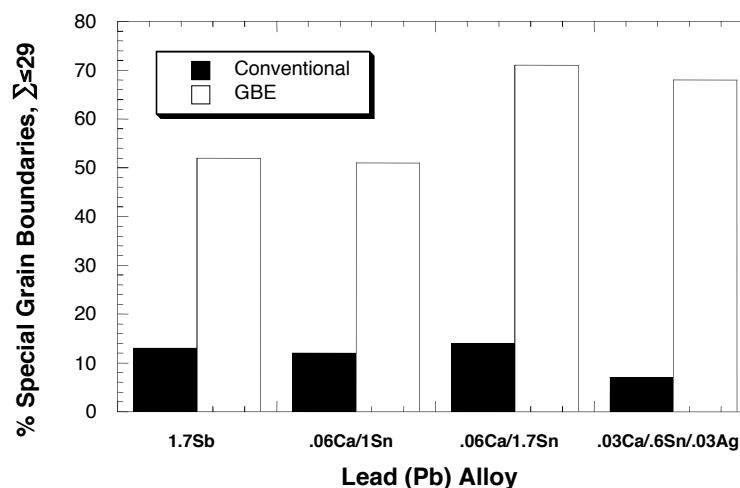


Conventional lead-acid battery grid (Pb-1wt%Sb) following 4 years of service.



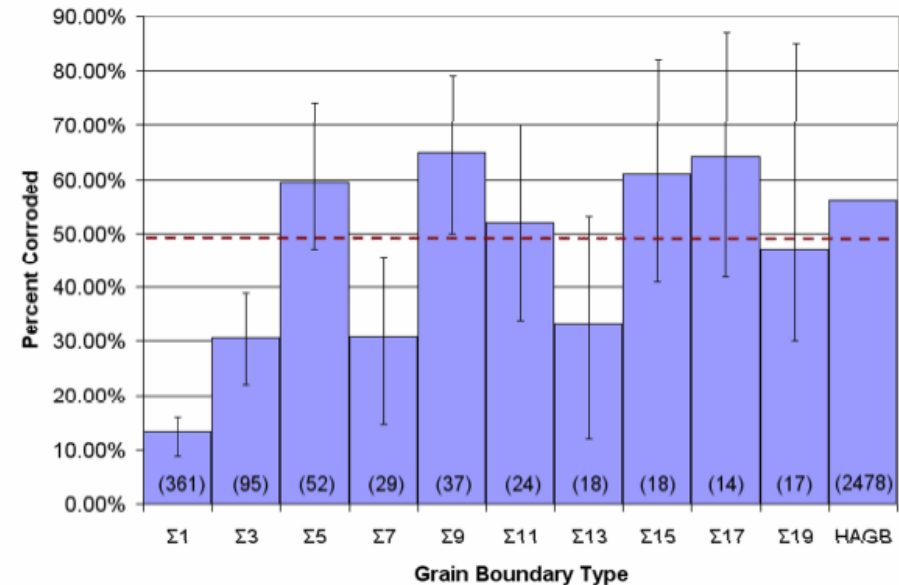
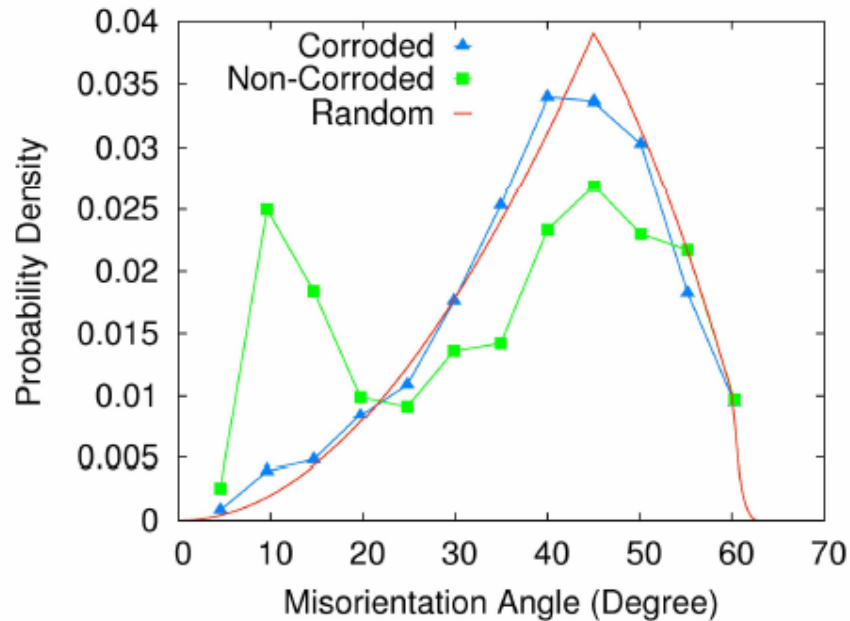
Conventional
 (fsp<15%) after
 2 weeks of
 cycling.

GBE
 (fsp=55%) after
 4 weeks of
 cycling.



Palumbo, G. *et al.* (1998). "Applications for grain boundary engineered materials." *Journal of Minerals, Metallurgy and Materials (JOM)* **50** 40-43.

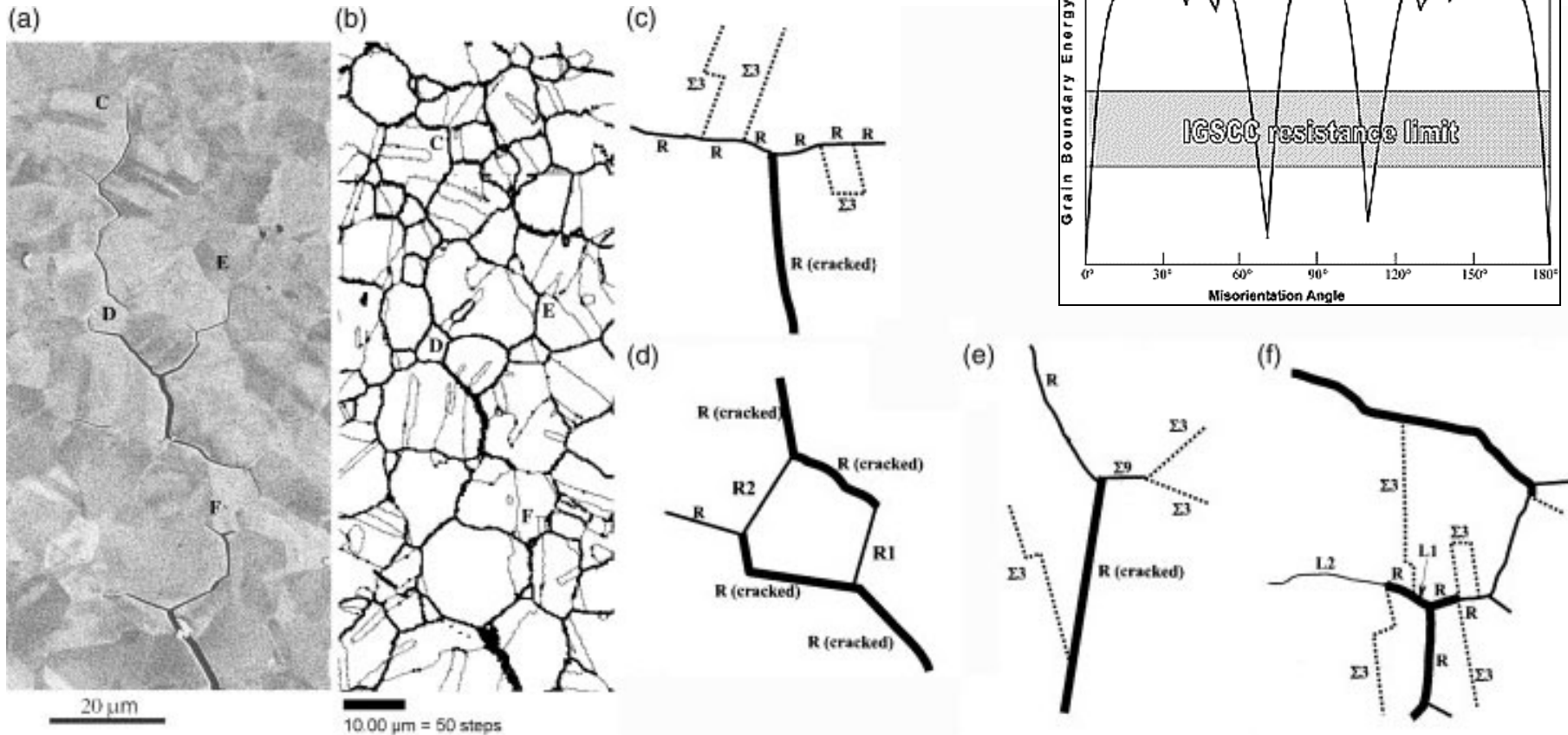
Corrosion of Aluminum 2124



- Results from experiment involving intergranular corrosion of aluminum alloy 2124. Low angle boundaries are measurably more resistant than high angle boundaries. Some evidence for resistance of $\Sigma 3$ and $\Sigma 7$ boundaries (possibly also $\Sigma 13$). Research by Lisa Chan, CMU.

Corrosion in Ni

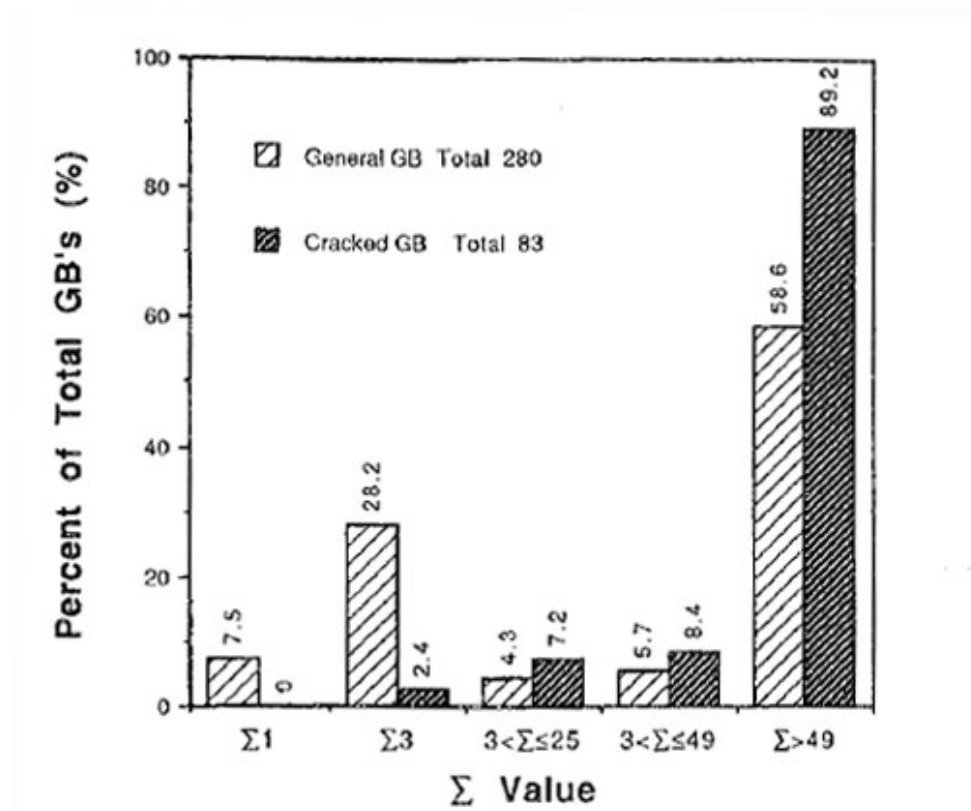
Alloy 600 (Ni-base alloy)



Several $\Sigma 3$ boundaries with larger deviations from ideal misorientation cracked.

Gertsman *et al.*, *Acta Mater.*, 49 (9): 1589-1598 (2001).

$\Sigma 3$ Boundaries



Ni_3Al

Cracked $\Sigma 3$ boundaries were found to deviate more than 5° from the trace of the $\{111\}$ plane.

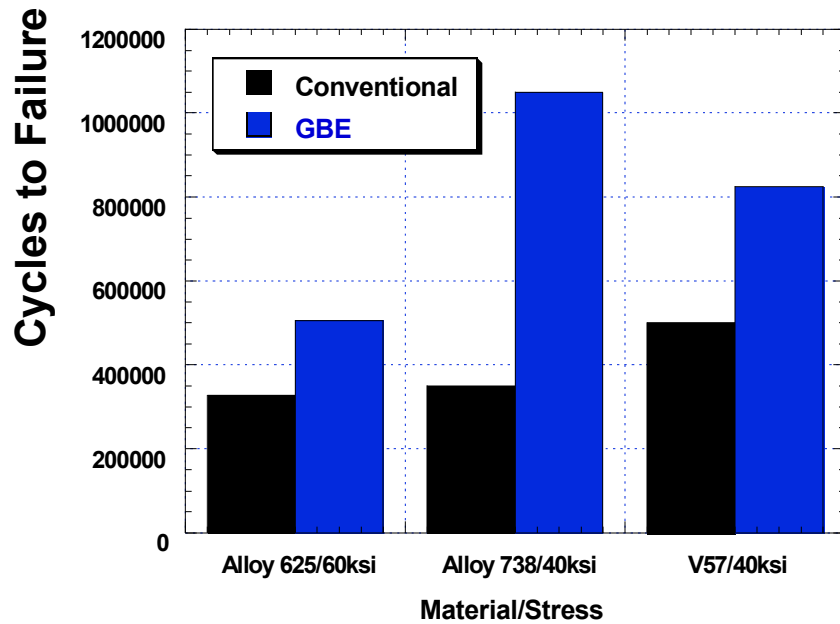
Lin *et al.*, *Acta Metall. Mater.*, **41** (2): 553-562 (1993).



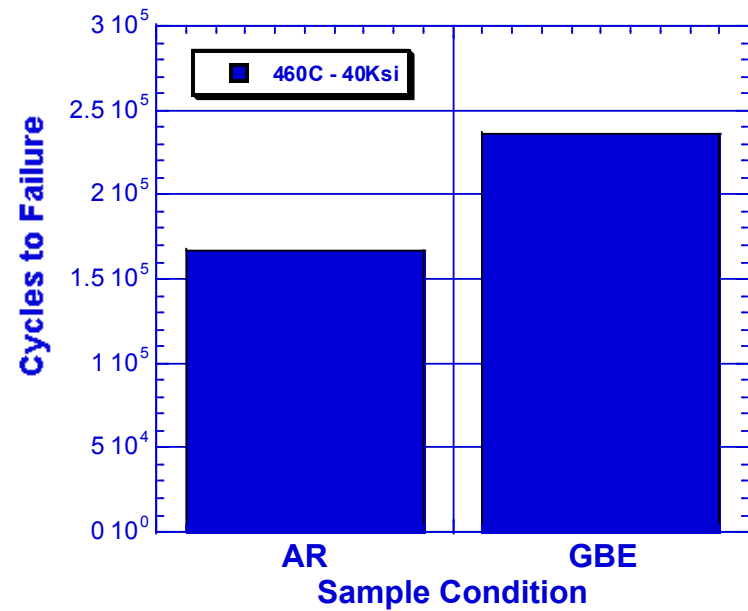
Fatigue



Room Temperature Fatigue Performance of Selected Nickel Based Alloys



Elevated Temperature Fatigue Performance of Alloy 625



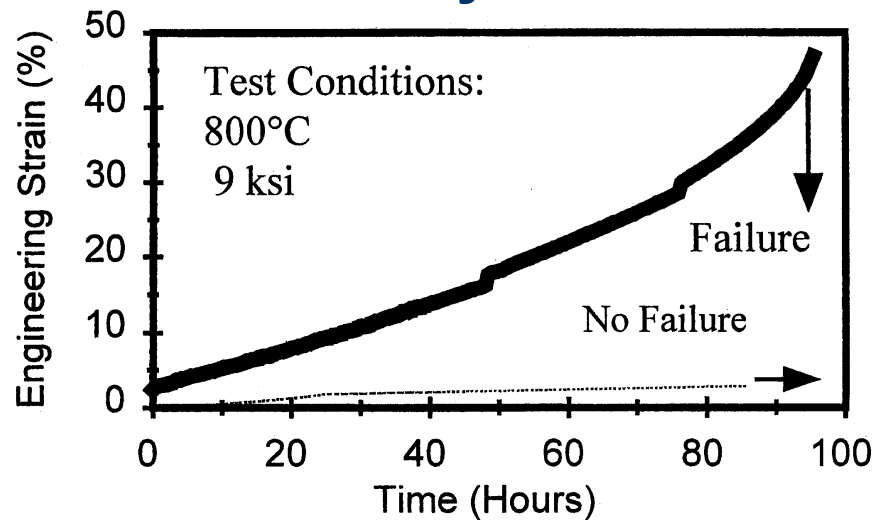


Creep

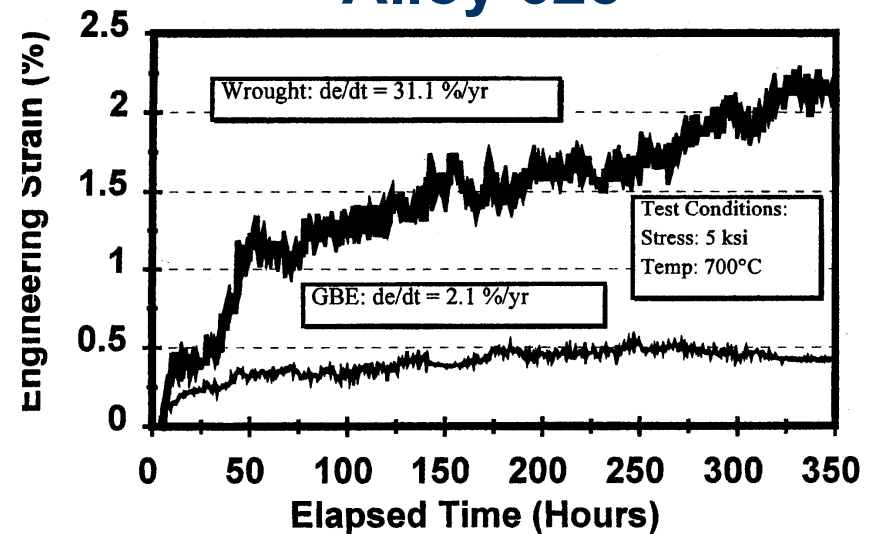


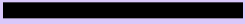
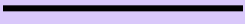
Thaveerungsriporn, V. and G. S. Was (1997). "The role of coincidence-site-lattice boundaries in creep of Ni-16Cr-9Fe at 360 degrees C." *Metallurgical And Materials Transactions A* 28(10): 2101; Alexandreanu, B. et al. (2003). "The effect of grain boundary character distribution on the high temperature deformation behavior of Ni-16Cr-9Fe alloys." *Acta materialia* 51 3831.

Alloy V57



Alloy 625



	Conventional
	GBE

Special Grain Boundaries

- There are some boundaries that have special properties, e.g. low energy.
- In most known cases (but not all!), these boundaries are also special with respect to their crystallography.
- When a finite fraction of lattice sites coincide between the two lattices, then one can define a coincident site lattice (CSL).
- A boundary that contains a high density of lattice points in a CSL is expected to have low energy because of good atomic fit.
- Note that the boundary plane matters, in addition to the misorientation; this means, in effect, that only pure tilt or pure twist boundaries are likely to have a high density of CSL lattice points.
- Relevant website:
http://www.tf.uni-kiel.de/matwis/amat/def_en/kap_7/illustr/a7_1_1.html (a page from a general set of pages on defects in crystals:
http://www.tf.uni-kiel.de/matwis/amat/def_en/index.html).

Grain Boundary properties

- For example, fcc $\langle 110 \rangle$ tilt boundaries show pronounced minima in energy
- However, some caution needed because the $\langle 100 \rangle$ series do *not* show these minima.

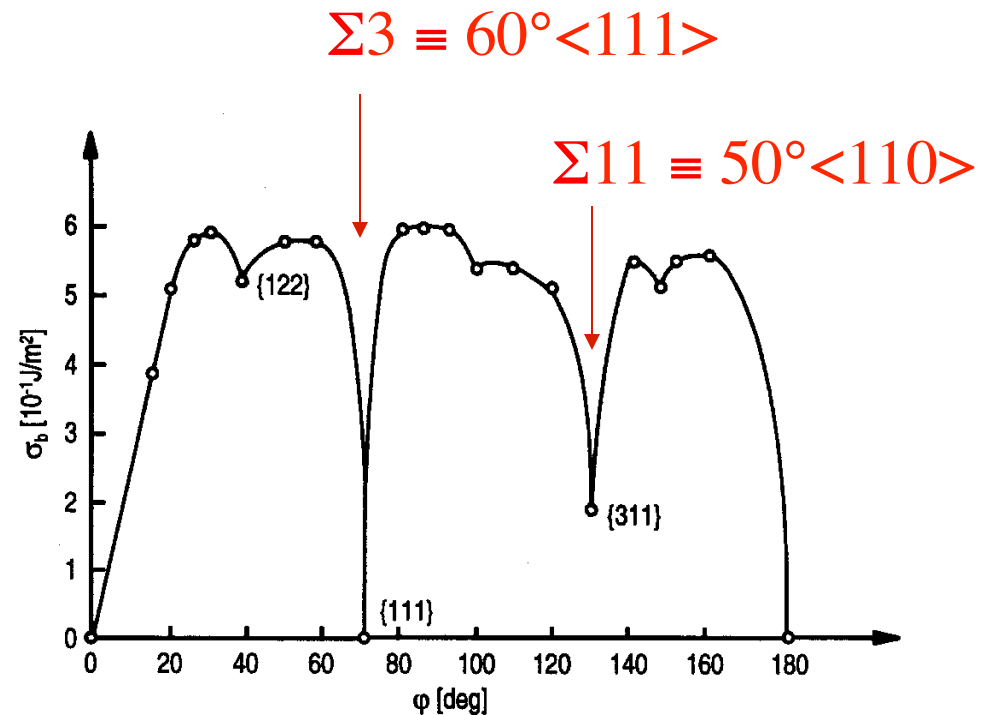


Fig. 2.4. Dependence of the energy of symmetrical $\langle 110 \rangle$ tilt boundaries in Al on the tilt angle ϕ . The indices given in the figure are Miller indices of the corresponding grain boundary planes (see text) (after [14]).

Figure taken from Gottstein & Shvindlerman, based on Goux, C. (1974). "Structure des joints de grains: consideration cristallographiques et methodes de calcul des structures." *Canadian Metallurgical Quarterly* **13**: 9-31.]

Kronberg & Wilson

- Kronberg & Wilson in 1947 considered coincidence patterns for atoms in the boundary planes (as opposed to the coincidence of lattice sites). Their atomic coincidence patterns for 22° and 38° rotations on the 111 plane correspond to the $\Sigma 13b$ and $\Sigma 7$ CSL boundary types. Note the significance of coincidence in the plane of the boundary.
- Friedel also explored CSL-like structures in a study of twins.

Kronberg, M. L. and F. H. Wilson (1949), "Secondary recrystallization in copper", *Trans. Met. Soc. AIME*, **185**, 501-514 (1947).

Friedel, G. (1926). *Lecons de Cristallographie* (2nd ed.). Blanchard, Paris.

Sigma=5,
36.9°
<100>

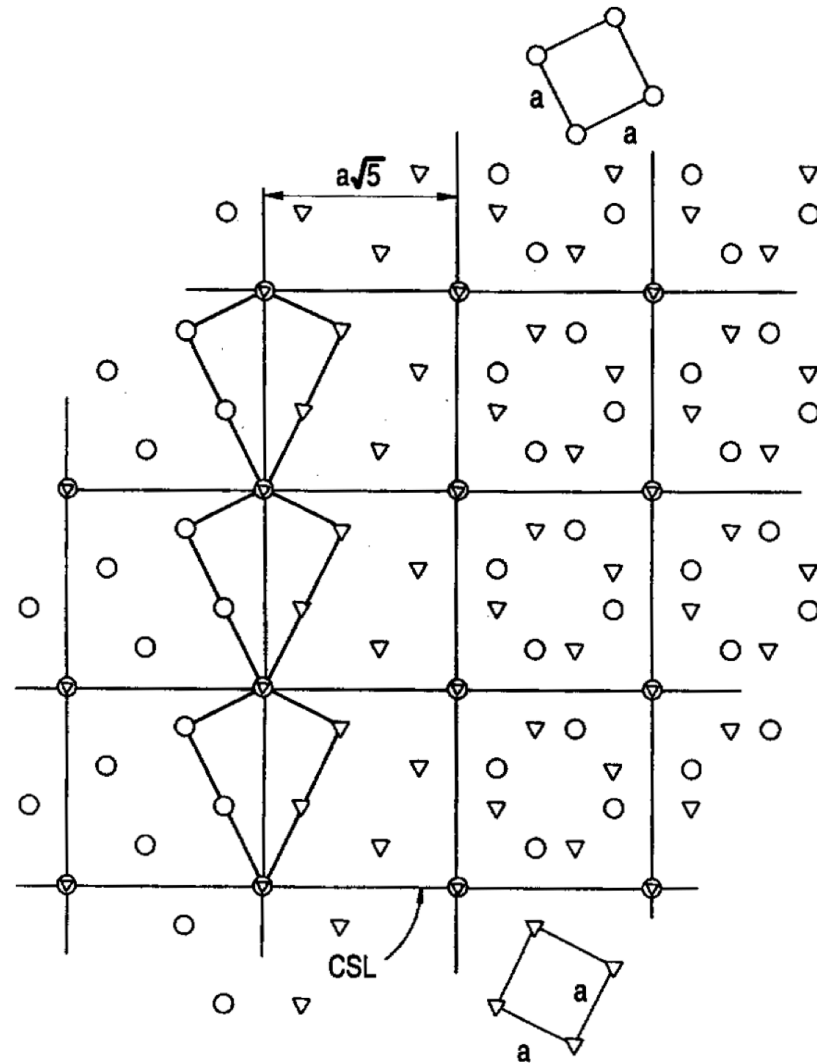


Fig. 2.10. Coincidence site lattice (CSL) and structure of a $36.9^\circ \langle 100 \rangle$ ($\Sigma=5$) grain boundary in a cubic crystal lattice. Right side of figure: grain boundary plane \parallel plane of the paper (twist boundary); Left side of figure: grain boundary plane \perp plane of the paper (tilt boundary).

[Sutton & Balluffi]

CSL = geometrical concept

- The CSL is a geometrical construction based on the geometry of the lattice.
- Lattices cannot actually overlap!
- If a (fixed) fraction of lattice sites are coincident, then the expectation is that the boundary structure will be more regular than a general boundary.
- Atomic positions are *not* accounted for in CSLs.
- It is possible to compute the density of coincident sites in the plane of the boundary - this goes beyond The basic CSL concept, which has to do only with the lattice misorientation.

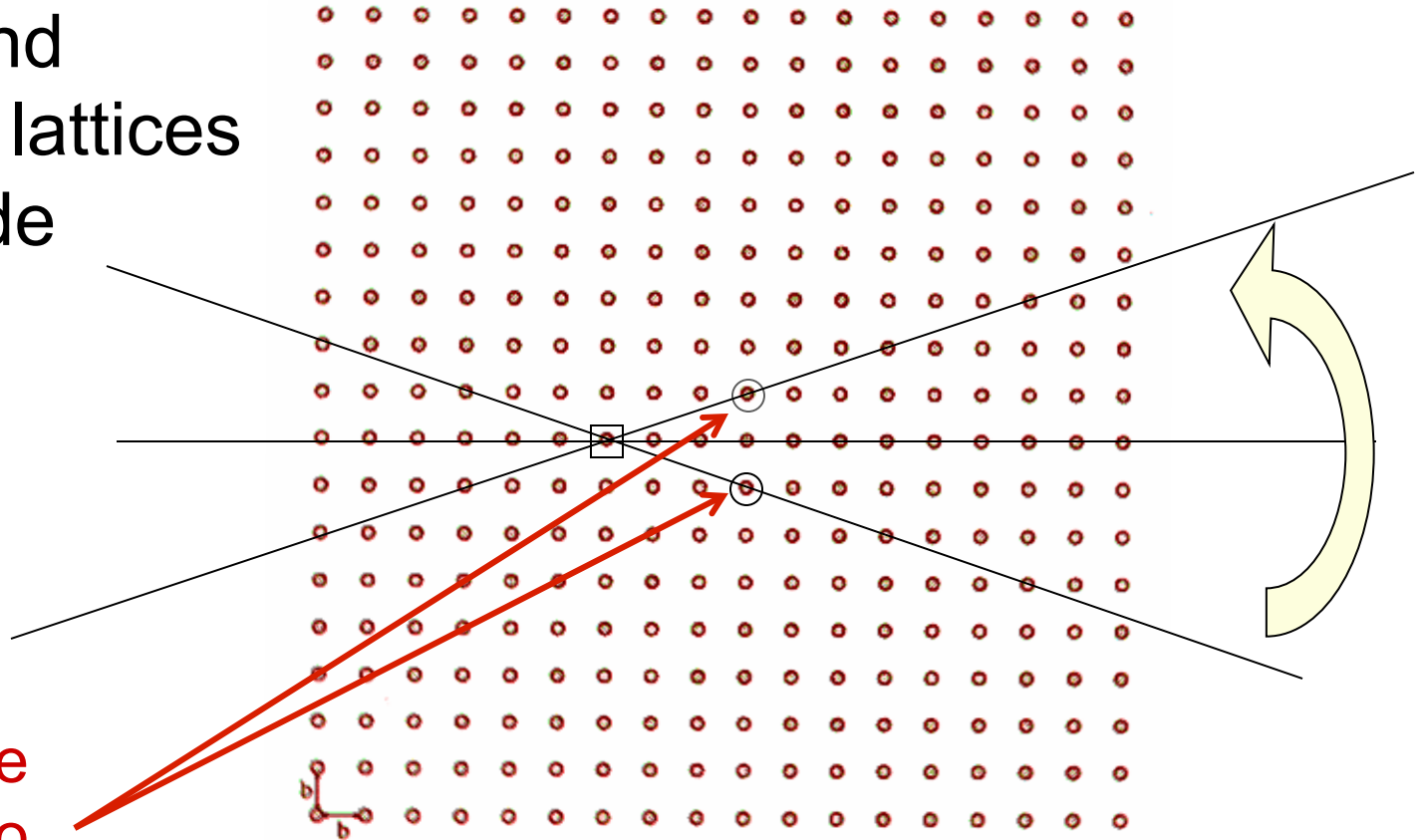
CSL construction

- The rotation of the second lattice is limited to those values that bring a (lattice) point into coincidence with a different point in the first lattice.
- The geometry is such that the rotated point (in the rotated lattice 2) and the superimposed point (in the fixed lattice 1) are related by a mirror plane in the unrotated state.

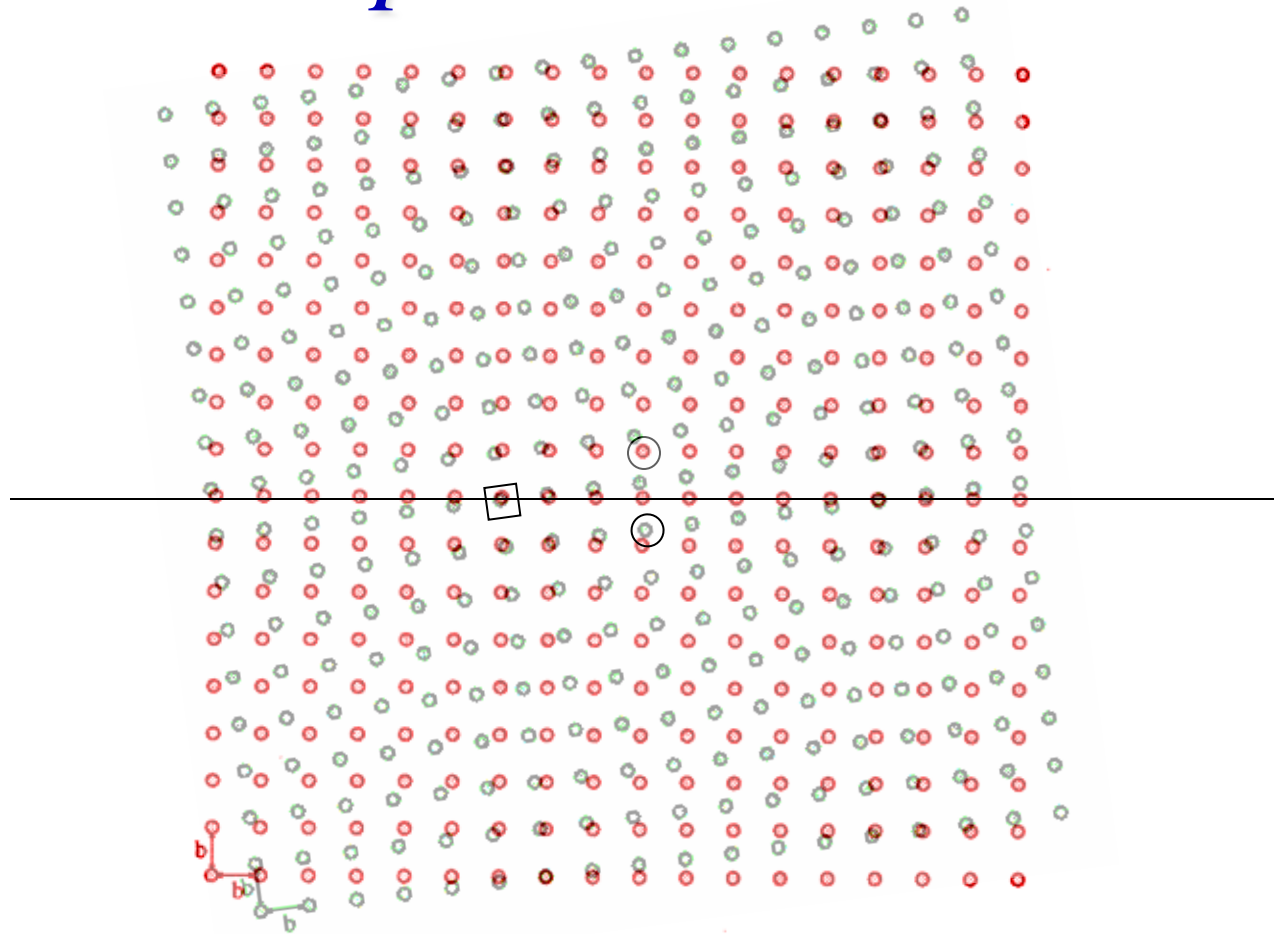
Rotation to Coincidence

- Red and Green lattices coincide

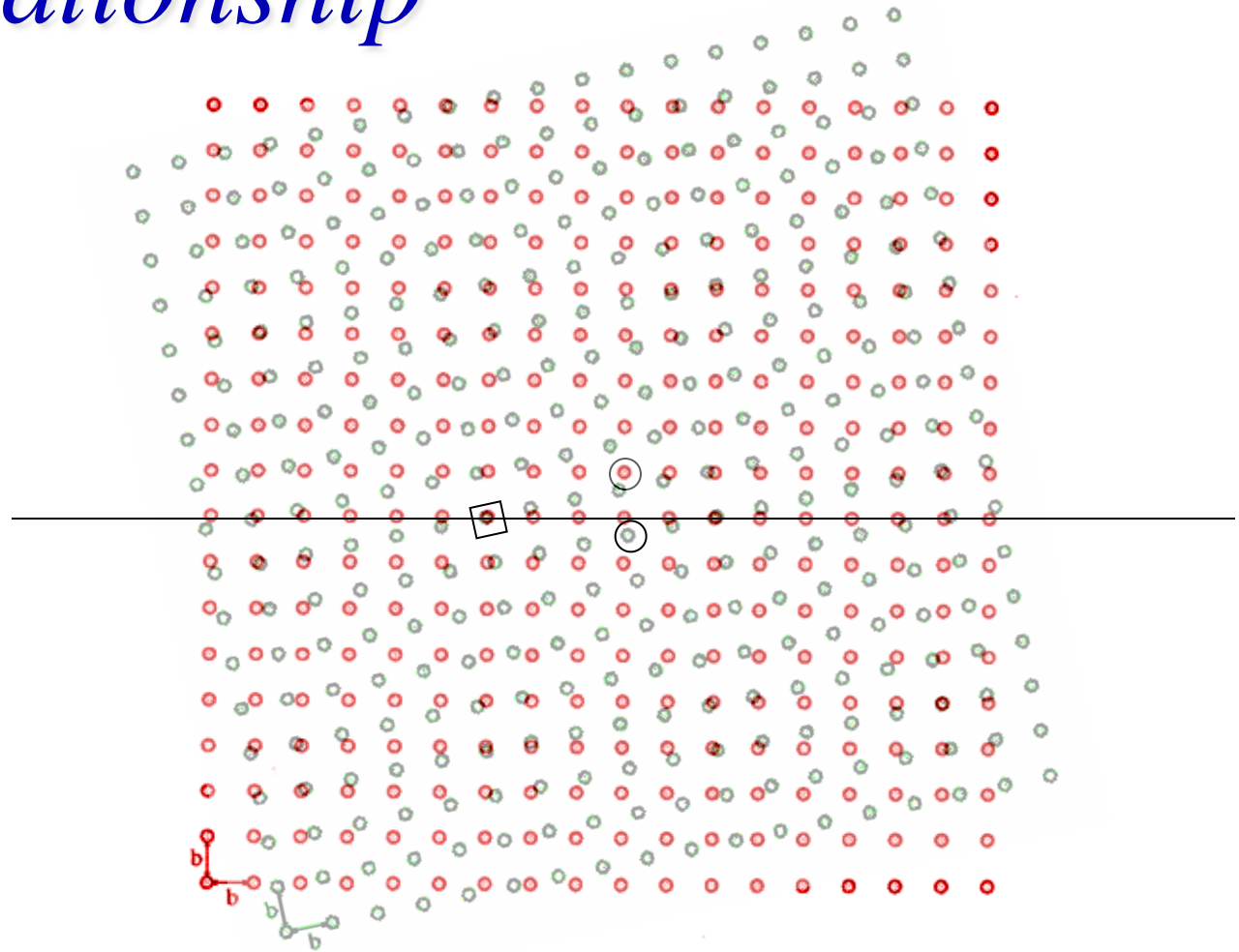
Points to be brought into coincidence



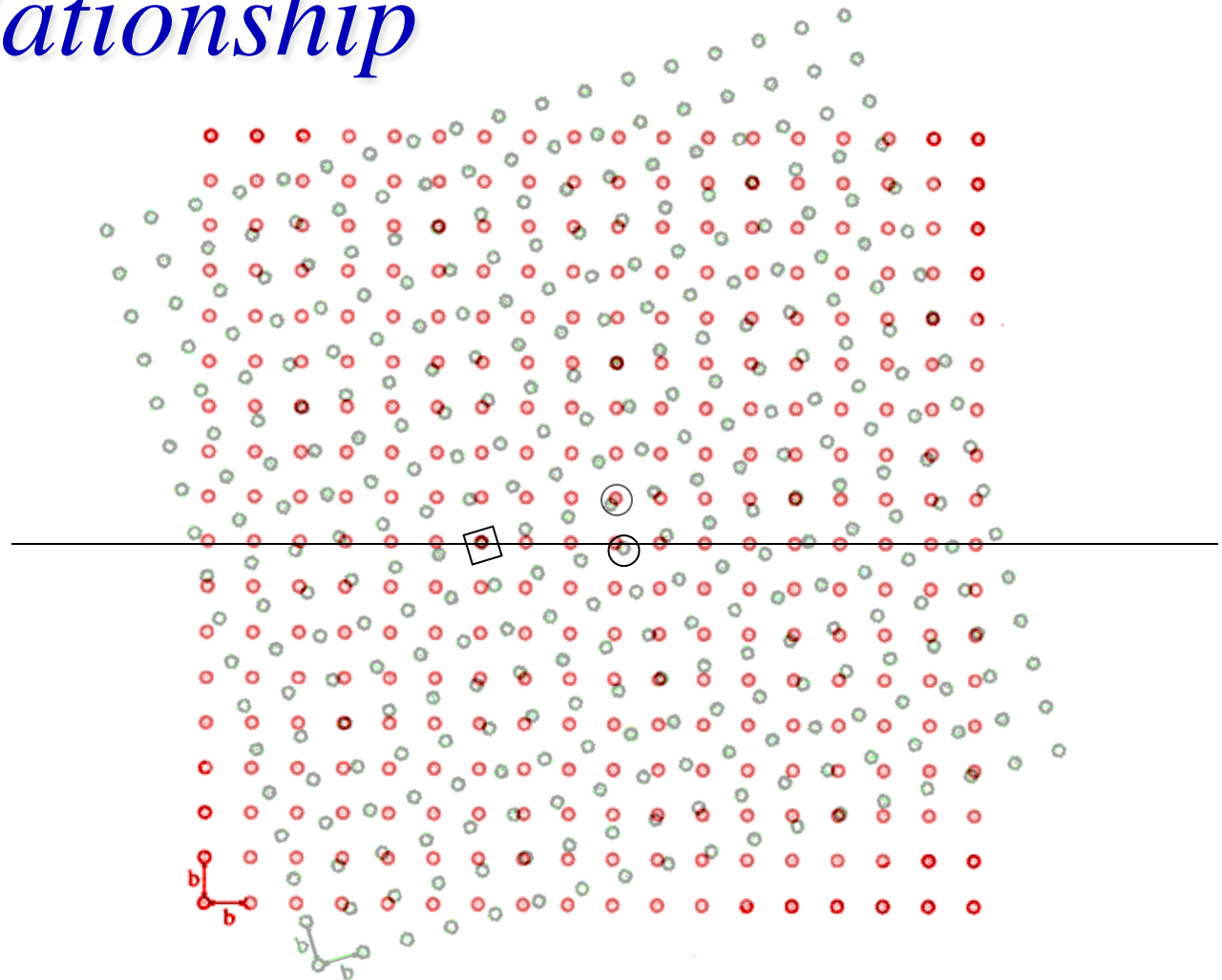
rotating to the $\Sigma 5$ relationship



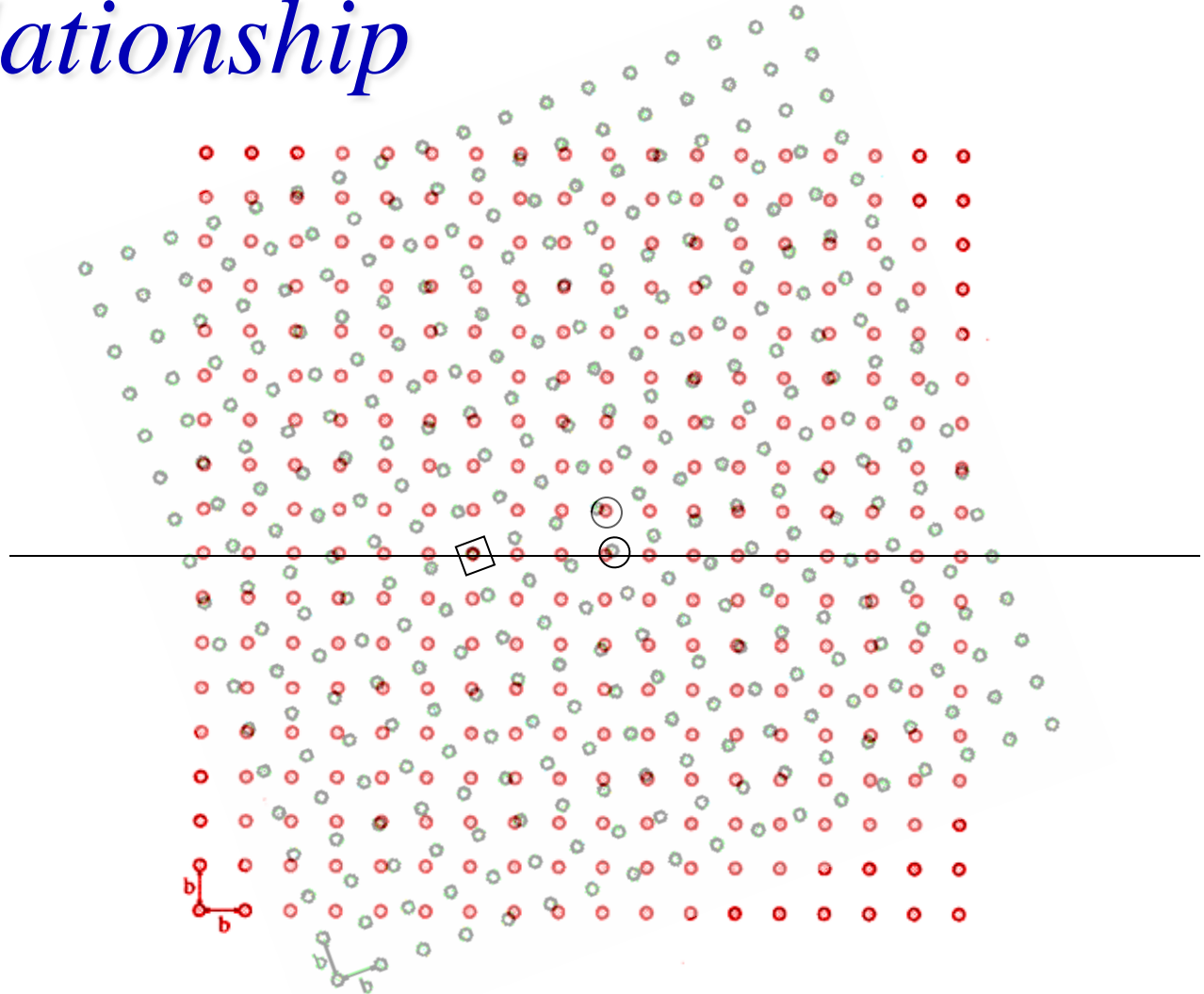
rotating to the $\Sigma 5$ relationship



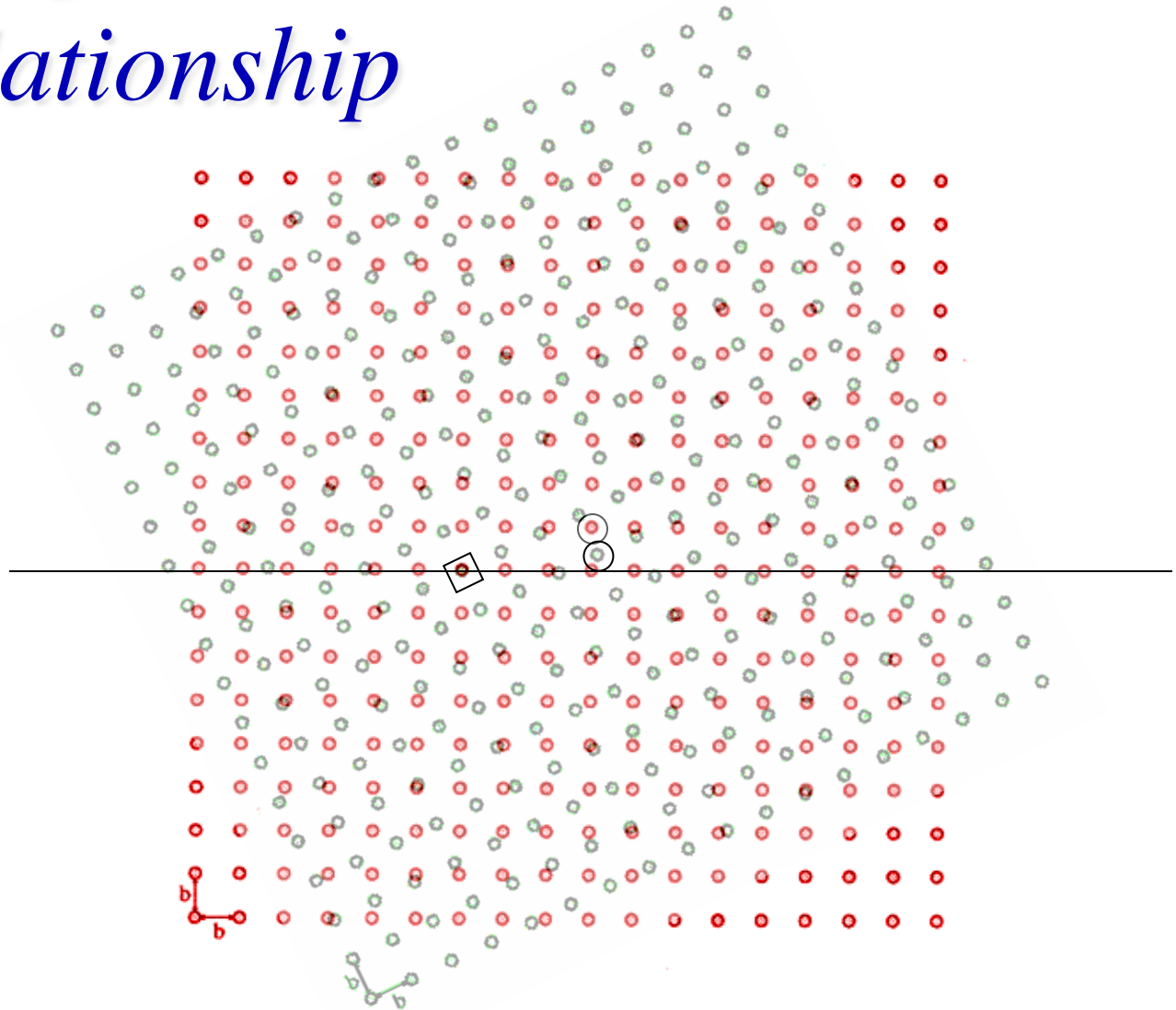
rotating to the $\Sigma 5$ relationship



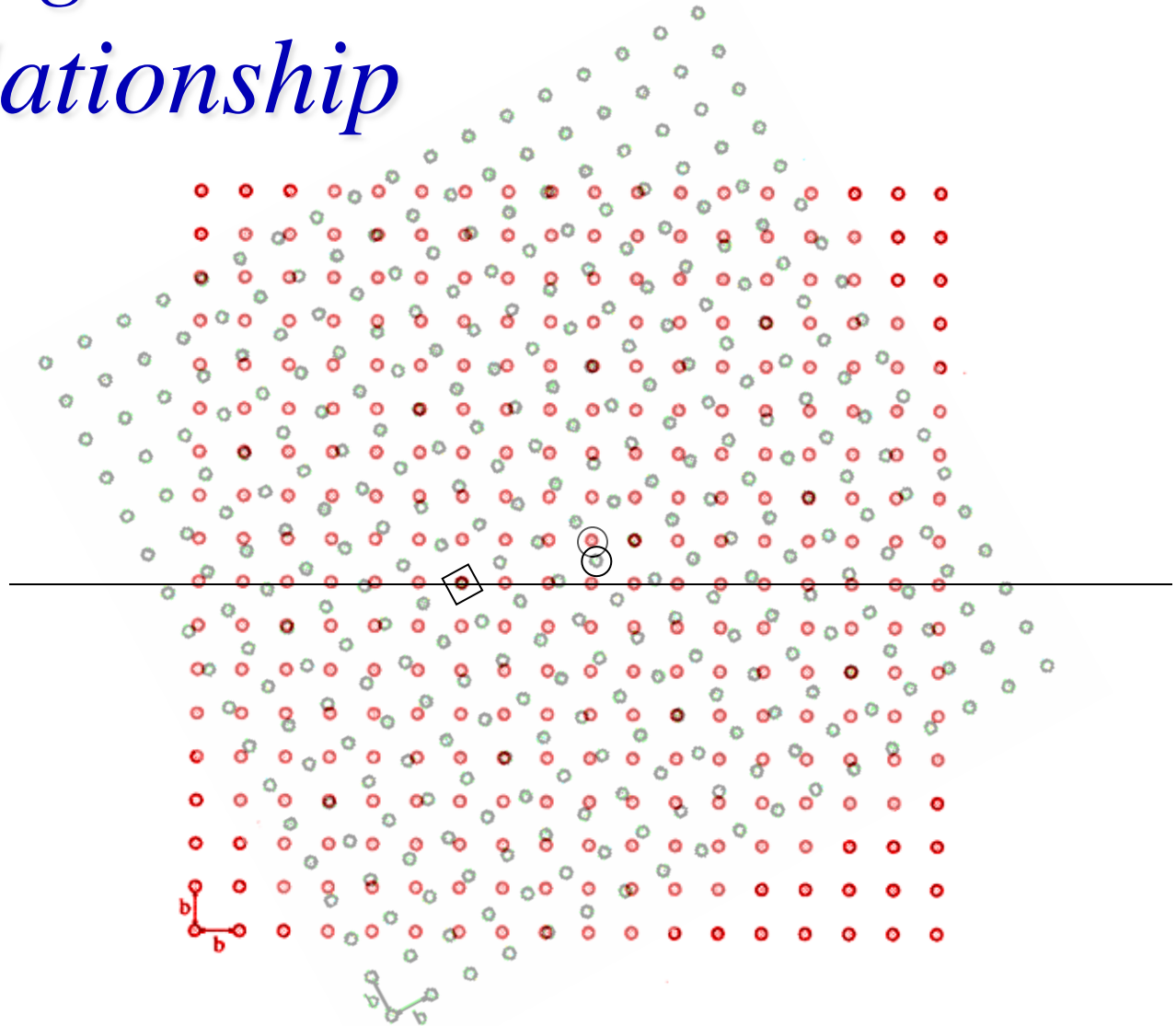
*rotating to the $\Sigma 5$
relationship*



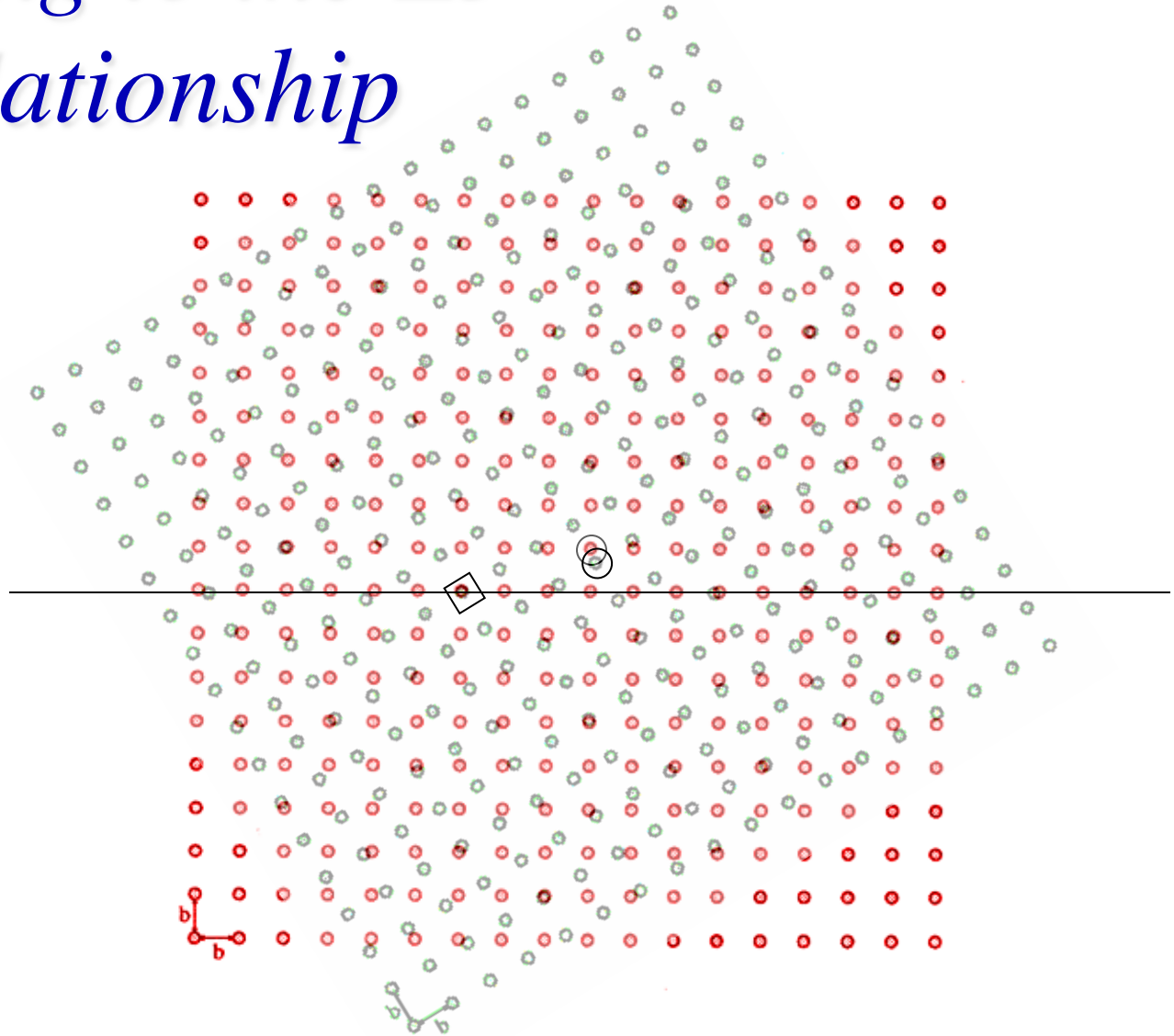
rotating to the $\Sigma 5$ relationship



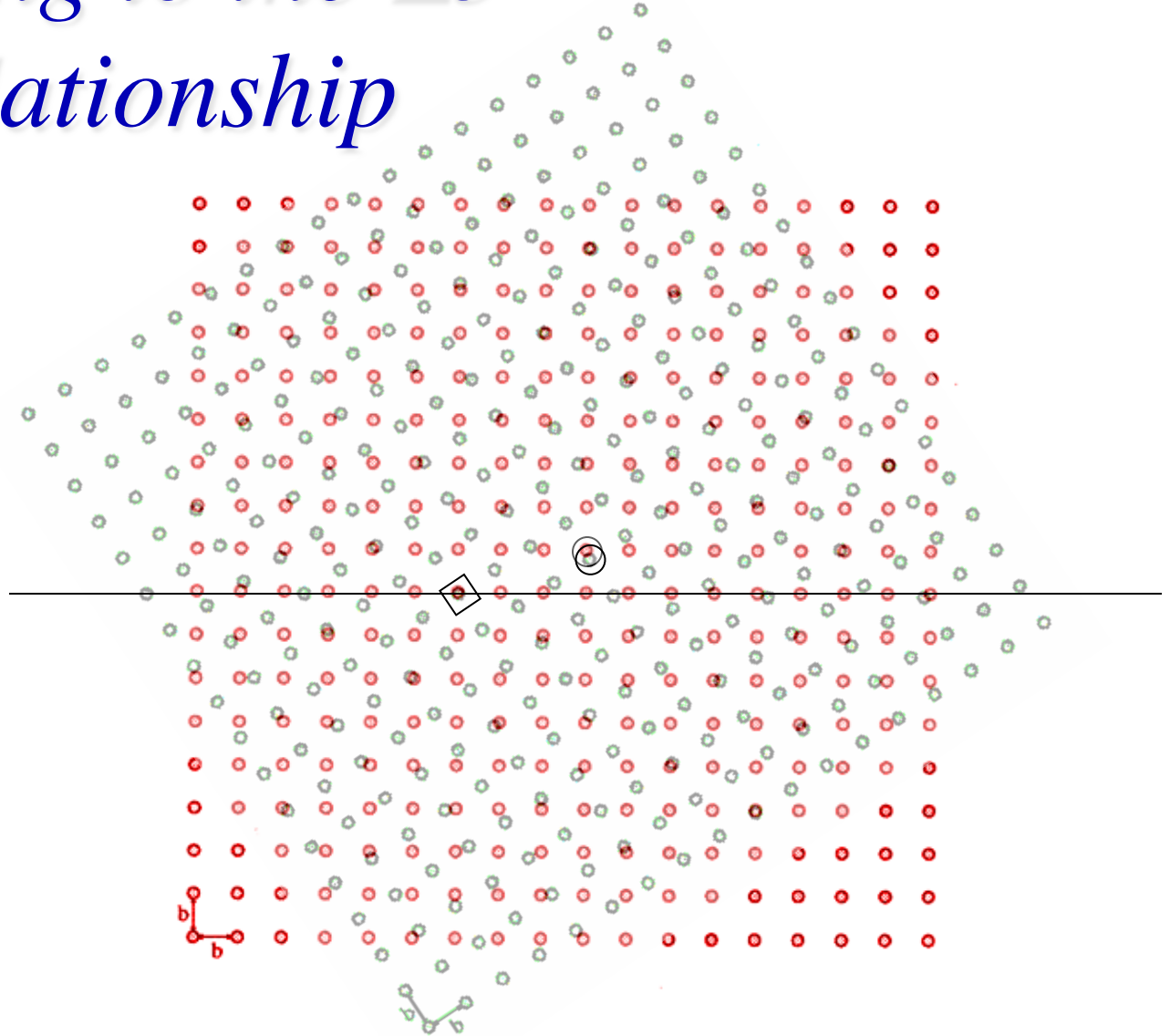
*rotating to the $\Sigma 5$
relationship*



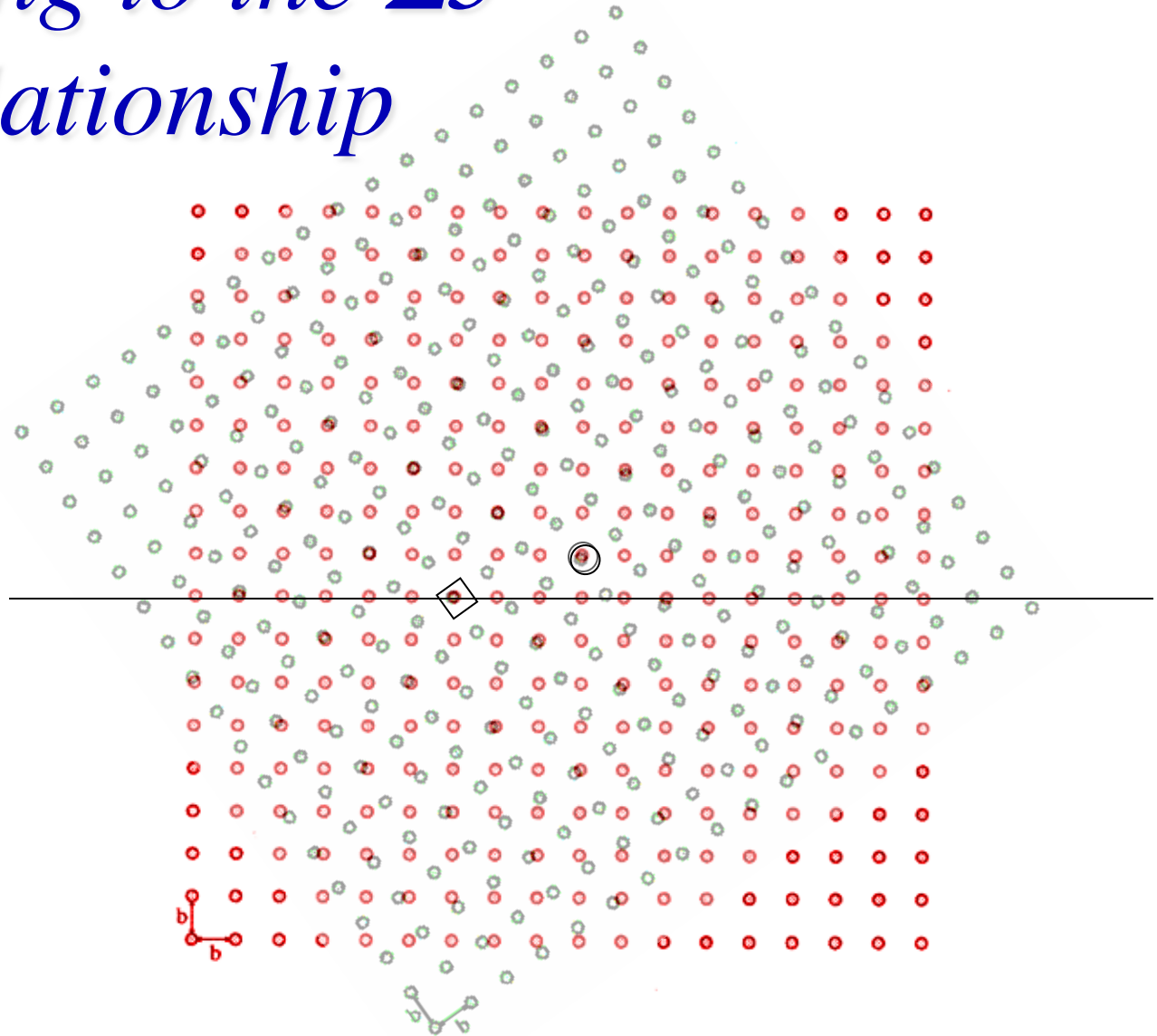
*rotating to the $\Sigma 5$
relationship*



*rotating to the $\Sigma 5$
relationship*

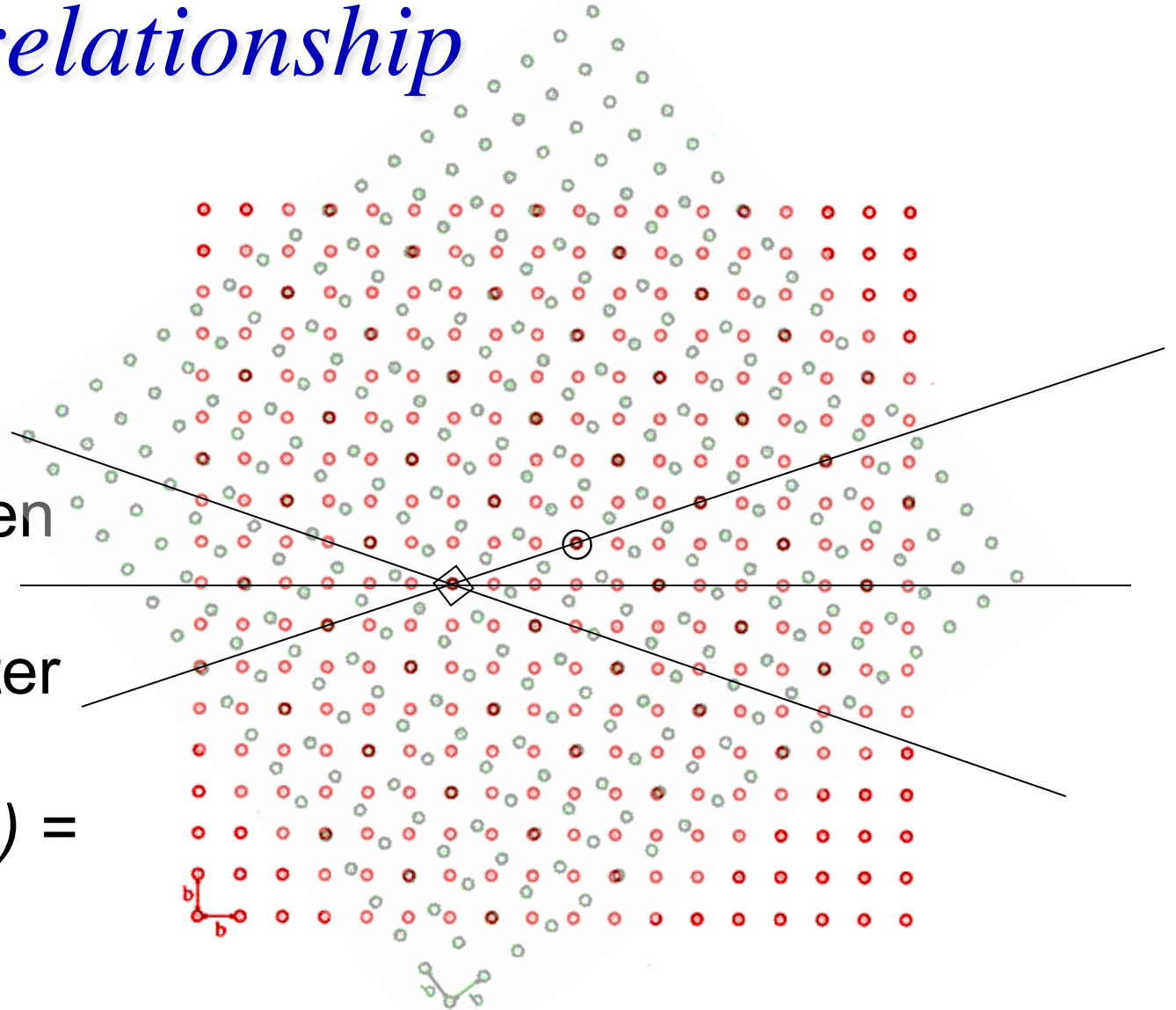


*rotating to the $\Sigma 5$
relationship*



$\Sigma 5$ relationship

Red and Green
lattices
coincide after
rotation of
 $2 \tan^{-1} (1/3) =$
 36.9°



Rotation to achieve coincidence

- Rotate lattice 1 until a lattice point in lattice 1 coincides with a lattice point in lattice 2.
- Clear that a higher density of points observed for low index axis.

[Bollmann, W. (1970). Crystal Defects and Crystalline Interfaces. New York, Springer Verlag.]

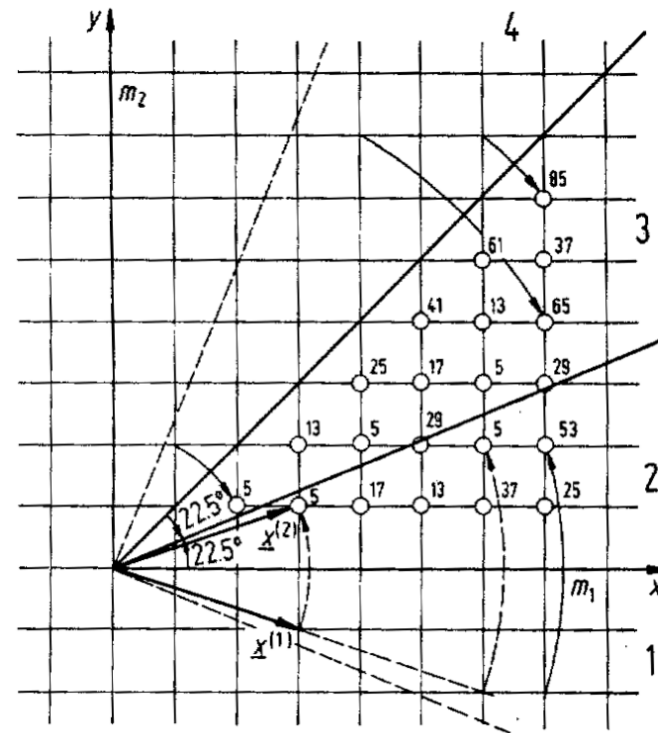


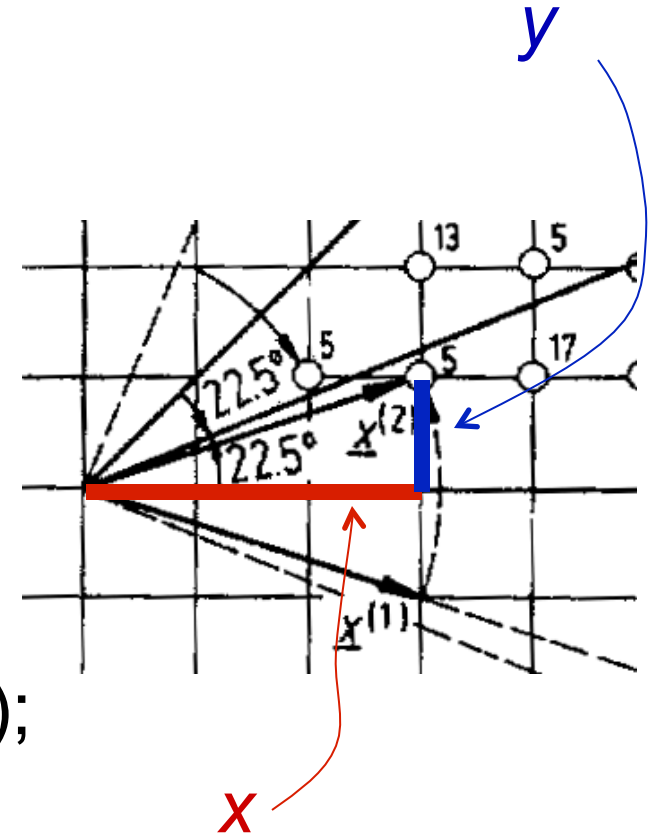
Fig. 12.2/1. Determination of the Σ -values for rotation on the $\{100\}$ -plane in the cubic structure (see Table 13.3/T1, No. 1–22)

CSL rotation angle

- The angle of rotation can be determined from the lattice geometry. The discrete nature of the lattice means that the angle is always determined as follows.

$$\theta = 2 \tan^{-1} (y/x),$$

where (x,y) are the coordinates of the superimposed point (in 1); x is measured parallel to the mirror plane.



CSL <-> Rodrigues

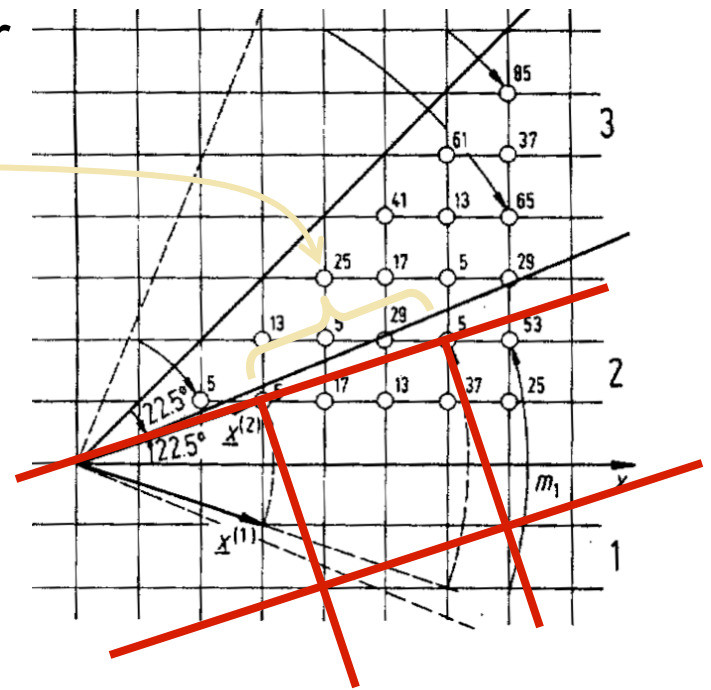
- You can immediately relate the angle to a Rodrigues vector because the tangent of the semi-angle of rotation must be rational (a fraction, y/x); thus the magnitude of the corresponding Rodrigues vector must also be rational!
- Example: for the $\Sigma 5$ relationship, $x=3$ and $y=1$; thus $\theta = 2 \tan^{-1} (y/x) = 2 \tan^{-1} (1/3) = 36.9^\circ$ and the rotation axis is $[1,0,0]$, so the complete Rodrigues vector = $[1/3, 0, 0]$.

The Sigma value (Σ)

- Define a quantity, Σ' , as the ratio between the area enclosed by a unit cell of the coincidence sites, and the standard unit cell. For the cubic case that whenever an even number is obtained for Σ' , there is a coincidence lattice site in the center of the cell which then means that the true area ratio, Σ , is half of the apparent quantity. Therefore Σ is always odd in the cubic system.

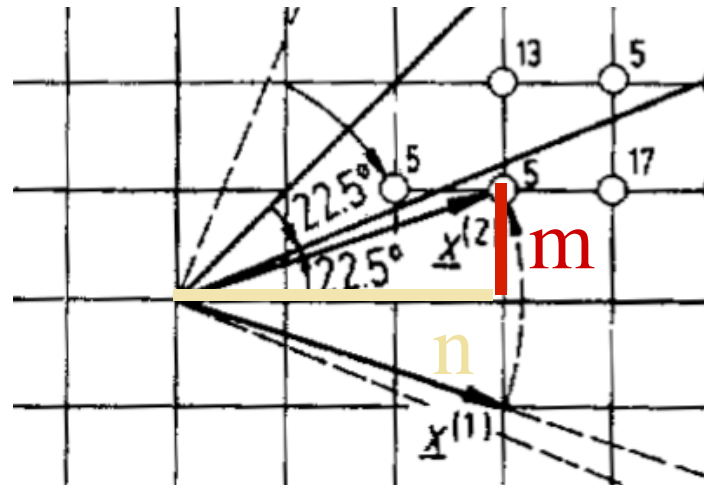
Generating function

- Start with a square lattice. Assign the coordinates of the coincident points as $(n,m)^*$: the new unit cell for the coincidence site lattice is square, each side is $\sqrt{m^2+n^2}$ long. Thus the area of the cell is m^2+n^2 . Correct for m^2+n^2 even: there is another lattice point in the center of the cell thereby dividing the area by two.
- * n and m are identical to x and y discussed in previous slides



Range of m, n

- Restrict the range of m and n such that $m < n$.
- If $n = m$ then all points coincide, and $m > n$ does not produce any new lattices.
- Example of $\Sigma 5$: $m = 1$, $n = 3$, area $= (3^2 + 1^2) = 10$; two lattice points per cell, therefore volume ratio = 1:5; rotation angle $= 2 \tan^{-1} 1/3 = 36.9^\circ$.



Generating function, contd.

- Generating function: we call the calculation of the area a *generating function*.

$$\Sigma = \begin{cases} 0.5(m^2 + n^2), & (m^2 + n^2) \text{ even} \\ m^2 + n^2, & (m^2 + n^2) \text{ odd} \end{cases}$$

Sigma denotes the ratio of the volume of coincidence site lattice to the regular lattice

Generating function: Rodrigues

- A rational Rodrigues vector can be generated by the following expression, where $\{m, n, h, k, l\}$ are all integers, $m < n$.

$$\boldsymbol{\rho} = m/n [h, k, l]$$

- The rotation angle is then:

$$\tan \theta/2 = m/n \sqrt{(h^2 + k^2 + l^2)}$$

Sigma Values

- A further useful relationship for CSLs is that for sigma. Consider the rotation in the (100) plane:

$$\tan\{\theta/2\} = m/n$$
- area of CSL cell = $m^2 + n^2$

$$= n^2 (1 + (m/n)^2) = n^2 (1 + \tan^2\{\theta/2\})$$
- Extending this to the general case, we can write:

$$\Sigma = n^2 (1 + \tan^2\{\theta/2\}) =$$

$$n^2 (1 + \{m/n \sqrt{(h^2 + k^2 + l^2)}\}^2) = n^2 + m^2(h^2 + k^2 + l^2)$$
- Note that although using these formulas and inserting low order integers generates most of the low order CSLs, one must go to values of $n \sim 5$ to obtain a complete list.

[Ranganathan, S. (1966). "On the geometry of coincidence-site lattices." [Acta Crystallographica](#) 21 197-199; see also the Morawiec book, pp 142-149 for discussion of cubic and lower symmetry cases]

Quaternions

- Recall that all CSL relationships can be thought of as twin relationships, which means that (in a centrosymmetric lattice) they can be constructed as 180° rotations about some axis.
- Rotations of 180° have a very simple representation as a quaternion (by contrast to Rodrigues vectors) because $\cos(\theta/2)=\cos(90^\circ)=0$ and $\sin(90^\circ)=1$. Therefore for a rotation axis of $[x,y,z]$ the unit quaternion = $\{x,y,z,0\}$.
- Take the $\Sigma 5$ as an example. The rotation axis is $[310]$, therefore the quaternion representation is $1/\sqrt{10}\{3,1,0,0\}$.
- Check that this is indeed the expected value by applying symmetry to the Δg and indeed one finds that this is equivalent to $\{1/3,0,0\}$ as a Rodrigues vector or $38.9^\circ[100]$.
- One can further check that a vector of type $[310]$ is mapped onto its negative by using the quaternion to transform/rotate it. If we choose $[-1,3,0]$ as being orthogonal to the $[310]$ axis, we can use the standard formula. PTO...

$$\mathbf{w} = (2q_0^2 - 1) \mathbf{v} + 2 (\mathbf{v} \cdot \mathbf{q}) \mathbf{q} + 2q_0 (\mathbf{v} \times \mathbf{q})$$

Quaternions, contd.

- Note that $q_0 = 0$ in these cases (of 180° rotations) and $\mathbf{q}^2=1$, so that simplifies the formula considerably:

$$\begin{aligned} s &= -\mathbf{v} + 2(\mathbf{v} \cdot \mathbf{q}) \mathbf{q} \\ &= -\mathbf{v} + 2(\mathbf{v} \cdot [310]) [310] \end{aligned}$$

- Pick $[-1,3,0]$ as an example:

$$\begin{aligned} &= -\mathbf{v} + 2([-1,3,0] \cdot [3,1,0]) [3,1,0] \\ &= -\mathbf{v} + 2([-3+3+0]) [3,1,0] \\ &= [+1,-3,0] \end{aligned}$$
- Note that any value of the z coefficient will *also* satisfy the relationship.
- Note that any combination of $b=-3a$ in $[a,b,c]$ (i.e. that has integer coordinates to be a point in the lattice, and is perpendicular to the axis) will also work. This helps to make the point that there is an infinite set of points that coincide, each of which satisfies the required relationship. That infinite set of coincident points is the Coincident Site *Lattice*.

Table of CSL values in axis/ angle, Euler angles, Rodrigues vectors and quaternions

Σ	θ (°)	uv w	ϕ_1, Φ, ϕ_2			ρ			q			
3	60	111	45	70.53	45	1/3	1/3	1/3	0.288	0.288	0.288	0.866
5	36.86	100	0	90	36.86	1/3	0.0	0.0	0.000	0.000	0.316	0.948
7	38.21	111	26.56	73.4	63.44	0.2	0.2	0.2	0.188	0.188	0.188	0.944
9	38.94	110	26.56	83.62	26.56	0.25	0.25	0.0	0.000	0.236	0.236	0.943
11	50.47	110	33.68	79.53	33.68	1/3	1/3	0.0	0.000	0.302	0.302	0.904
13a	22.62	100	0	90	22.62	0.2	0.0	0.0	0.000	0.000	0.196	0.981
13b	27.79	111	18.43	76.66	71.57	0.143	0.143	0.143	0.139	0.139	0.139	0.971
15	48.19	210	19.65	82.33	42.27	0.4	0.2	0.0	0.000	0.183	0.365	0.913
17a	28.07	100	0	90	28.07	0.25	0.0	0.0	0.000	0.000	0.243	0.970
17b	61.9	221	45	86.63	45	0.4	0.4	0.2	0.171	0.343	0.343	0.858
19a	26.53	110	18.44	89.68	18.44	1/6	1/6	0.0	0.000	0.162	0.162	0.973
19b	46.8	111	33.69	71.59	56.31	0.25	0.25	0.25	0.229	0.229	0.229	0.918
21a	21.78	111	14.03	79.02	75.97	1/9	1/9	1/9	0.109	0.109	0.109	0.982
21b	44.41	211	22.83	79.02	50.91	1/3	1/6	1/6	0.154	0.154	0.308	0.926
23	40.45	311	15.25	82.51	52.13	1/3	1/9	1/9	0.104	0.104	0.313	0.938
25a	16.26	100	0	90	16.26	0.143	0.0	0.0	0.000	0.000	0.142	0.99
25b	51.68	331	36.87	90	53.13	1/3	1/3	1/9	0.100	0.300	0.300	0.9
27a	31.59	110	21.8	85.75	21.8	0.2	0.2	0.0	0.000	0.193	0.193	0.962
27b	35.43	210	15.07	85.75	31.33	0.285	0.143	0.0	0.000	0.136	0.272	0.953
29a	43.6	100	0	90	43.6	0.4	0.0	0.0	0.000	0.000	0.393	0.928
29b	46.4	221	33.69	84.06	56.31	0.286	0.286	0.143	0.131	0.263	0.263	0.919
31a	17.9	111	11.31	80.72	78.69	1/11	1/11	1/11	0.09	0.09	0.09	0.988
31b	52.2	211	27.41	78.84	43.66	0.4	0.2	0.2	0.180	0.18	0.359	0.898
33a	20.1	110	12.34	83.04	58.73	0.125	0.125	0.000	0.000	0.123	0.123	0.985
33b	33.6	311	37.51	76.84	37.51	0.273	0.091	0.091	0.087	0.087	0.261	0.957
33c	59.0	110	38.66	75.97	38.66	0.4	0.4	0.000	0.000	0.348	0.348	0.870
35a	34.0	211	16.86	80.13	60.46	0.25	0.125	0.125	0.119	0.119	0.239	0.956
35b	43.2	331	30.96	88.36	59.04	0.272	0.272	0.091	0.083	0.253	0.253	0.93

Note: in order to compare a measured misorientation with one of these values, it is necessary to compute the values to high precision (because most are fractions based on integers).

Note: integer fractions are quoted for most of the Rodrigues vectors. The entries in decimals also correspond to integer values and will be updated at a later time.

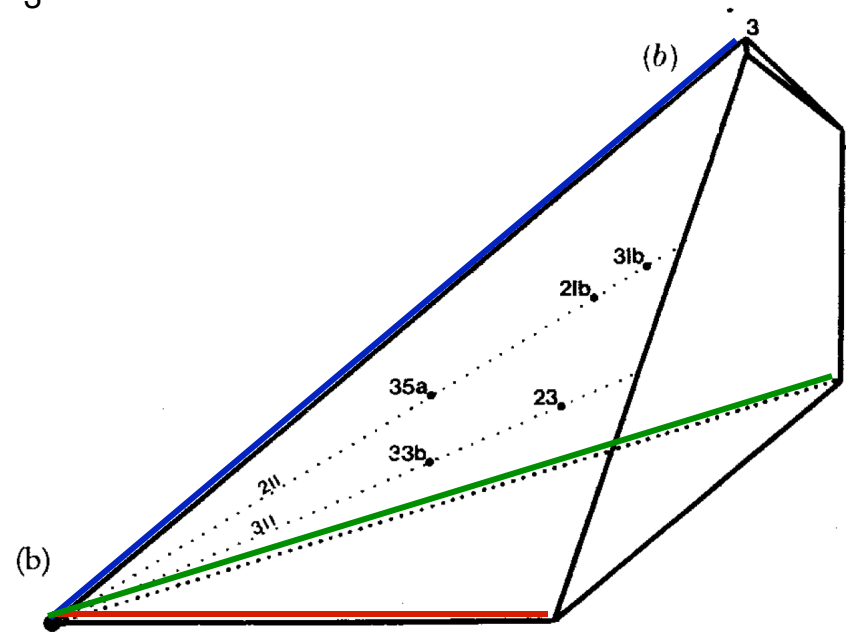
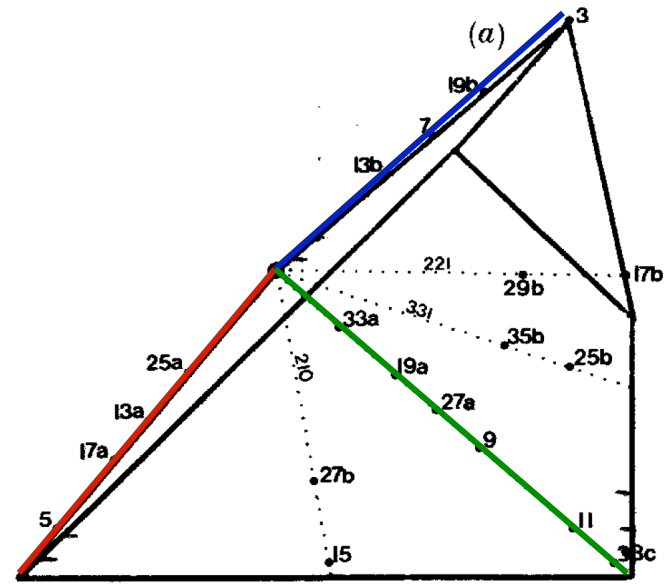
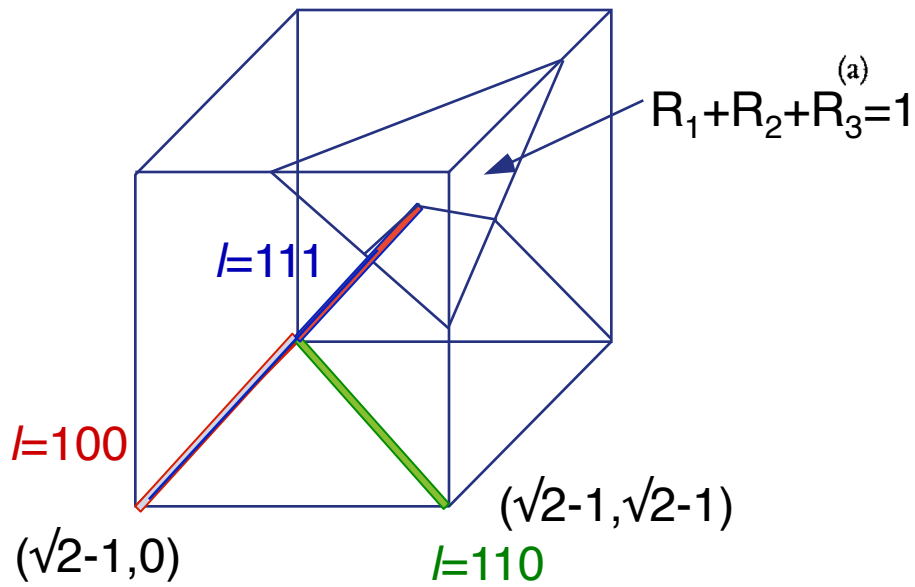
CSL + boundary plane

- Good atomic fit at an interface is expected for boundaries that intersect a high density of (coincident site) lattice points.
- How to determine these planes for a given CSL type?
- The coincident lattice is aligned such that one of its axes is parallel to the misorientation axis. Therefore there are two obvious choices of boundary plane to maximize the density of CSL lattice points:
 - (a) a *pure twist* boundary with a normal // misorientation axis is one example, e.g. (100) for any $\langle 100 \rangle$ -based CSL;
 - (b) a *symmetric tilt* boundary that lies perpendicular to the axis and that bisects the rotation should also contain a high density of points. Example: for $\Sigma 5$, 36.9° about $\langle 001 \rangle$, $x=3$, $y=1$, and so the (310) plane corresponds to the $\Sigma 5$ *symmetric tilt boundary plane* [i.e. $(n,m,0)$].

CSL boundaries and RF space

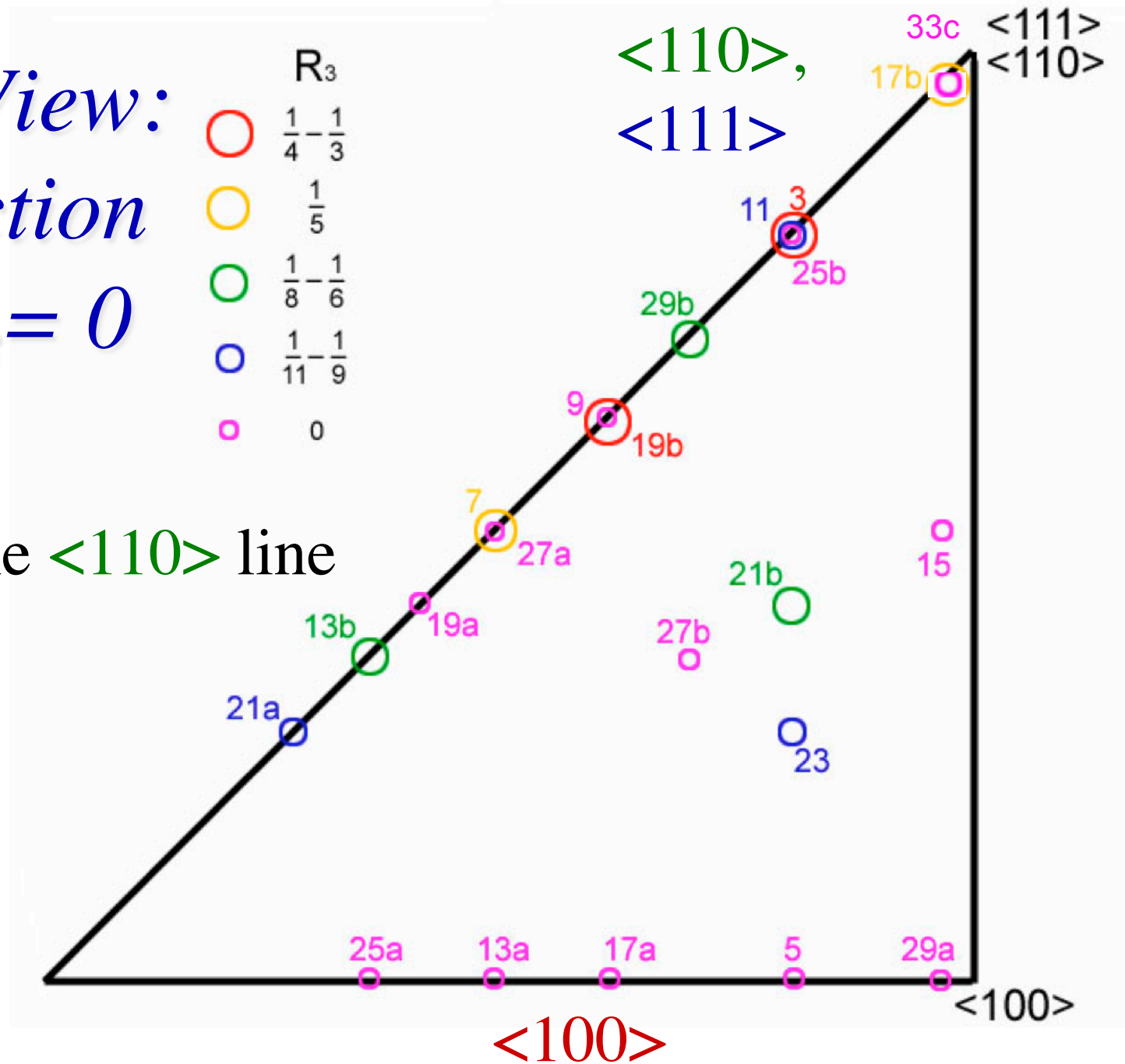
- The coordinates of nearly all the low-sigma CSLs are distributed along low index directions, i.e. $\langle 100 \rangle$, $\langle 110 \rangle$ and $\langle 111 \rangle$. Thus nearly all the CSL boundary types are located on the edges of the space and are therefore easily located.
- There are some CSLs on the 210, 331 and 221 directions, which are shown in the interior of the space.

RF pyramid and CSL locations



*Plan View:
Projection
on $R_3 = 0$*

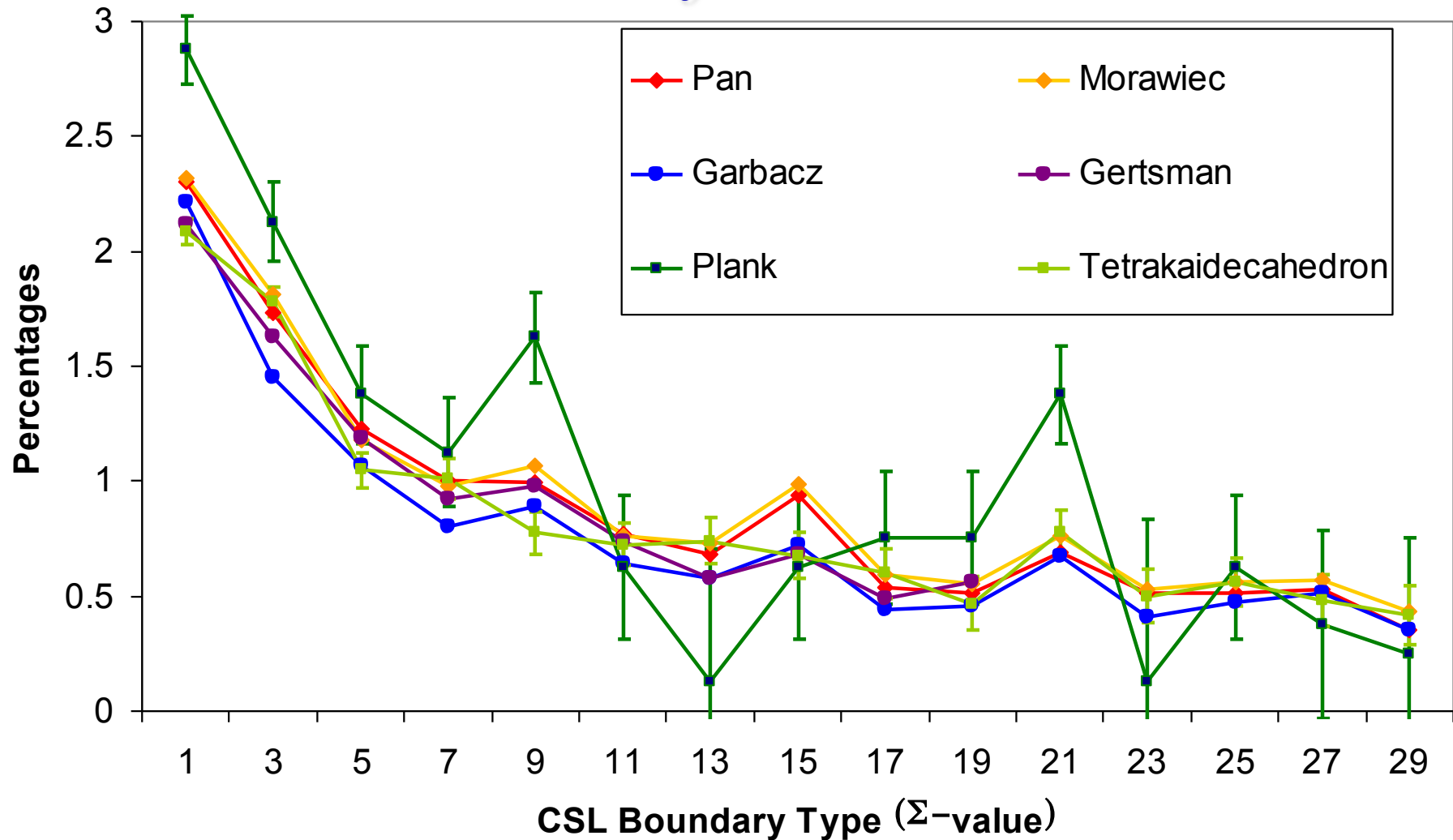
$\langle 111 \rangle$ line
lies over the $\langle 110 \rangle$ line



Fractions of CSL Boundaries in a Randomly Oriented Microstructure

- It is interesting is to ask what fraction of boundaries correspond to each sigma value in a randomly oriented polycrystal?
- The method to calculate such (area) fractions is exactly the same as for volume fractions in an Orientation Distribution.
- The Brandon Criterion establishes the “capture radius” for each sigma value (which decreases with increasing sigma value).
- All points (in a discretized MD) are assigned to a given CSL type if they fall within the capture radius.

CSL % for Random Texture



Garbacz *et al.*, *Scr. Mater.*, **23** (8): 1369-1374 (1989).

Gertsman *et al.*, *Acta Metall. Mater.*, **42** (6): 1785-1804 (1994).

Morawiec *et al.*, *Acta Metall. Mater.*, **41** (10): 2825-2832 (1993).

Pan *et al.*, *Scr. Metall. Mater.*, **30** (8): 1055-1060 (1994).

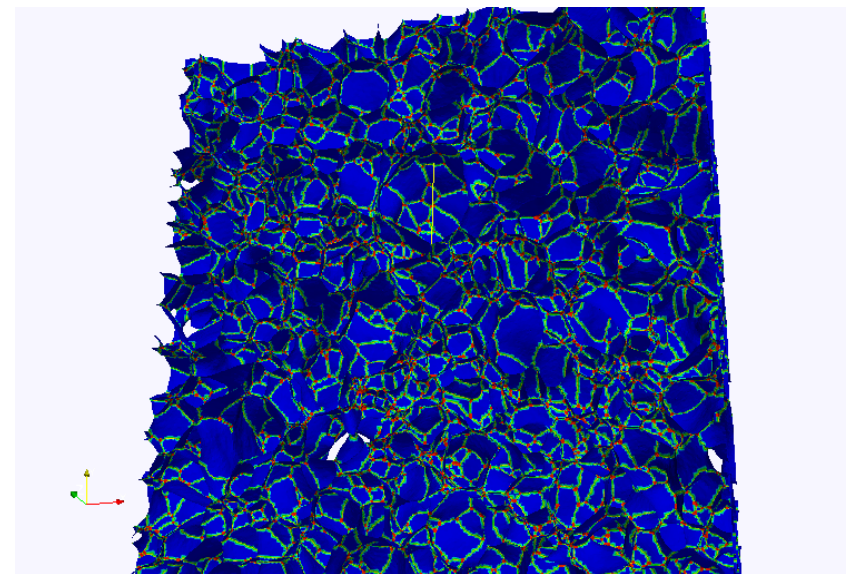
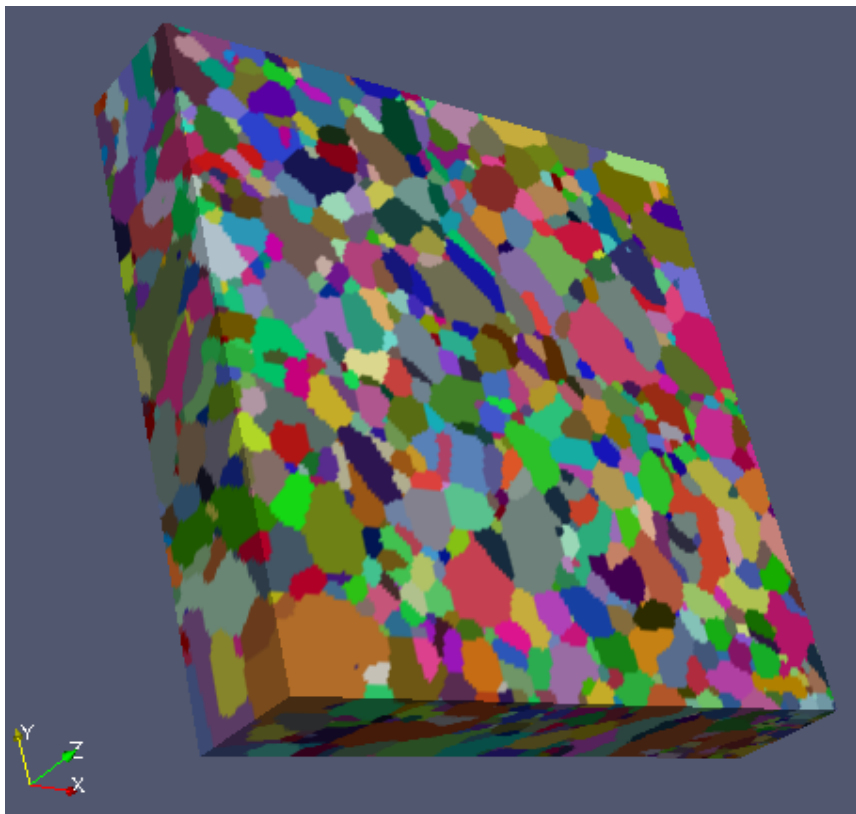
Generate MD from a random texture; analyze for fraction near each CSL type (method to be discussed later).

Grain Boundaries from High Energy Diffraction Microscopy

Measurements made at the Advanced Photon Source:

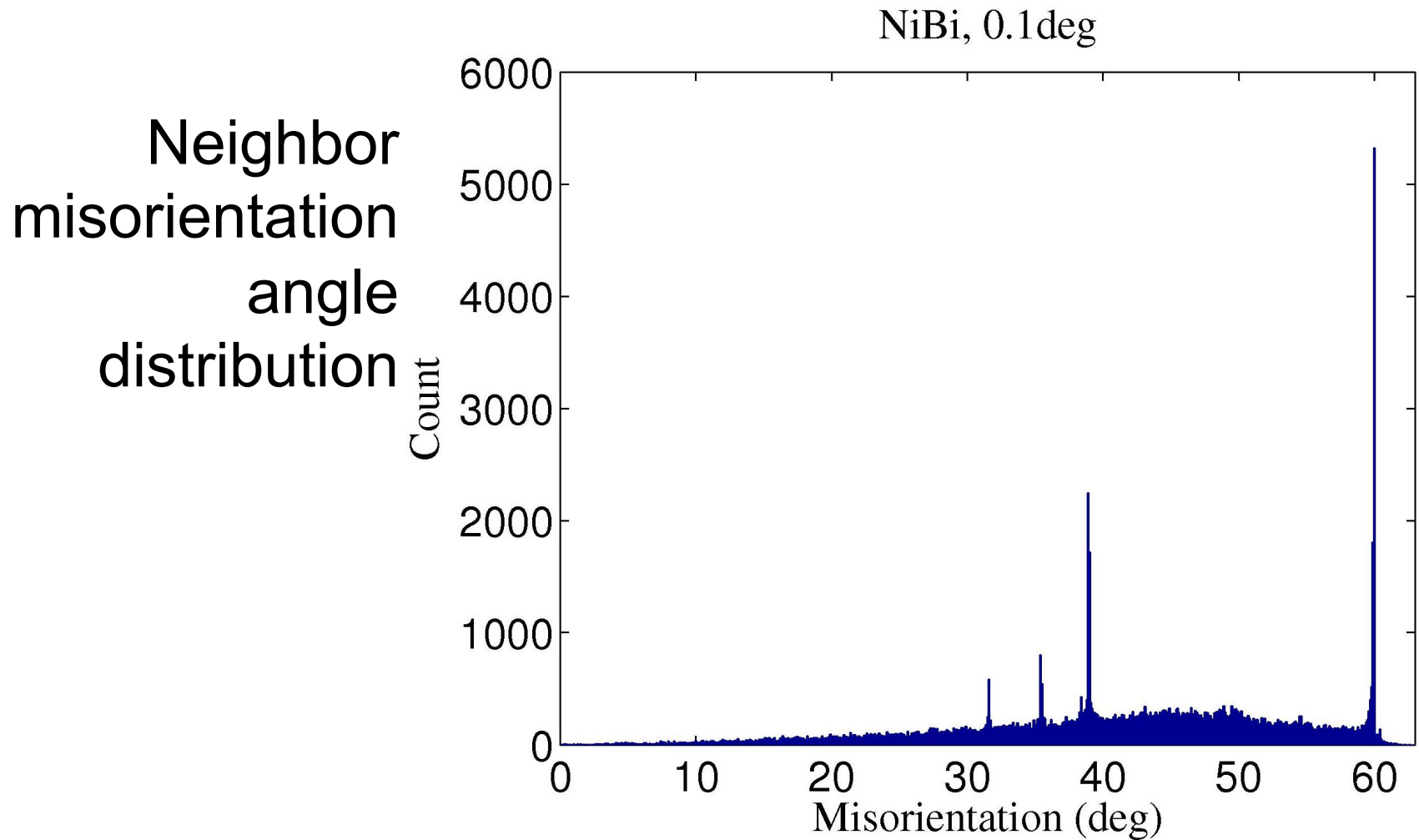
see [Hefferan *et al.* \(2009\). CMC 14 209-219.](#)

Pure Nickel: 42 layers, 4 micron spacing, 0.16 mm³



Pure Ni sample, 42 layers
3,496 grains; ~ 23,598 GBs

Statistics extraction from large data sets

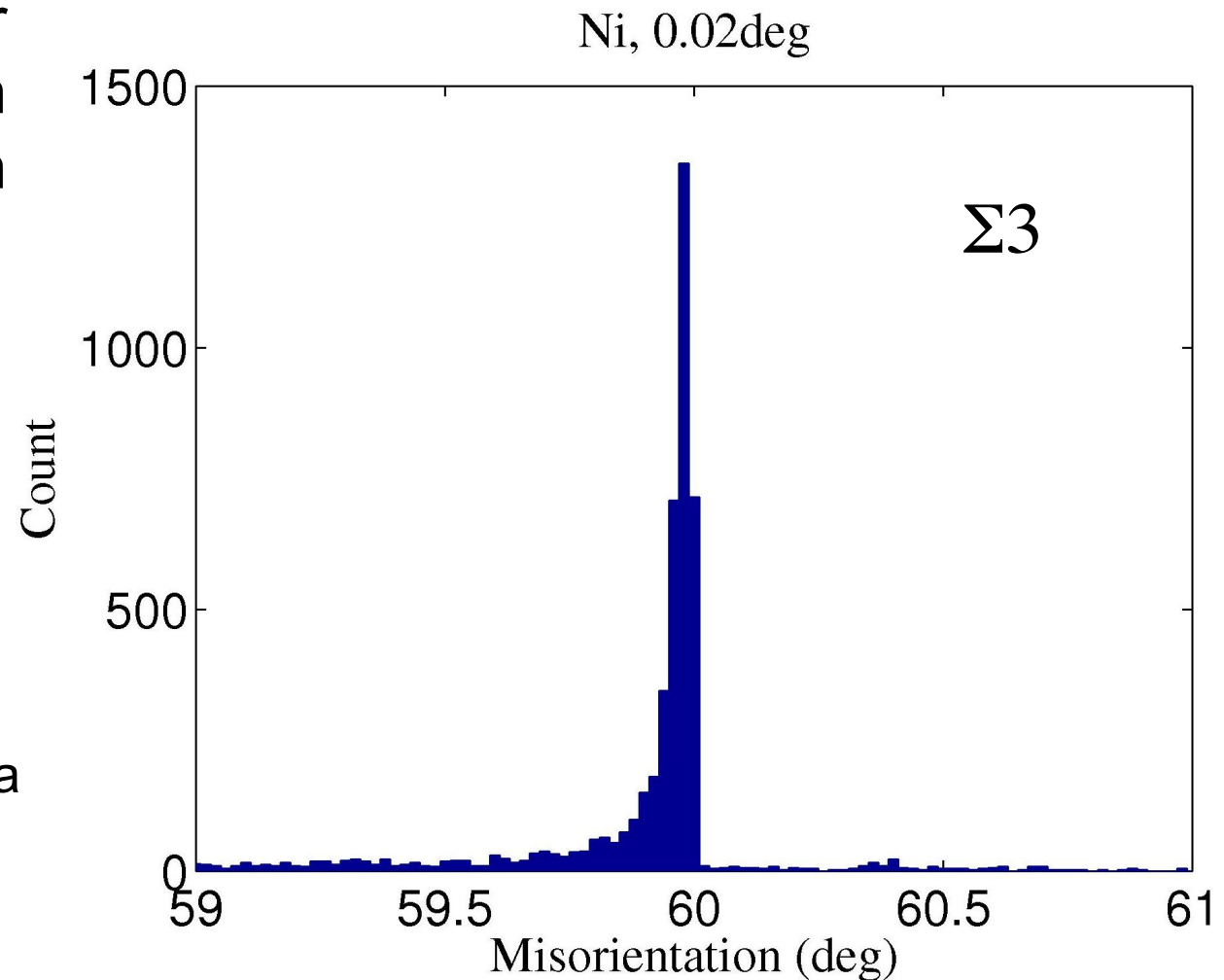


Hefferan *et al.* (2009). CMC 14 209-219.

Statistics extraction from large data sets

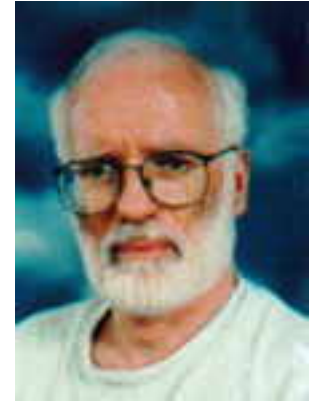
Neighbor
misorientation
angle distribution

Conclusion:
The misorientations
of grain boundaries
in these nickel
samples are
concentrated on a
small number of
CSL types, i.e. sigma
= 3,7,9,11,27



Hefferan *et al.* (2009). CMC 14 209-219.

Brandon Criterion



- David Brandon [1966: "The structure of high-angle grain boundaries", *Acta metallurgica* 14: 1479-1484] originated a criterion for proximity to a CSL structure.

$$v_m = v_0 \Sigma^{1/2}$$

where the proportionality constant, v_0 , is generally taken to be 15° , based on the low-to-high angle transition.

- Larger sigma values imply larger unit cells in the boundary, fewer coincident points, larger dislocation densities for the same deviation from the exact CSL misorientation. Thus one has to be closer to the exact CSL position in order for a given boundary to be counted as belonging to that CSL type.
- Closeness to a misorientation type is defined by the angle associated with the rotation between the misorientation in question, Δg , and the CSL misorientation, Δg_{CSL} .

$$\cos(\theta_m) = \{\text{trace}(\Delta g \Delta g_{CSL}^T) - 1\} / 2$$

Impact of the Brandon Criterion

ISI Web of KnowledgeSM Web of Science



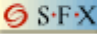
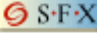
Search Results -- Summary

AU=(brandon dg)
DocType=All document types; Language=All languages; Database=SCI-EXPANDED; Timespar

119 results found (Set #1) Go to

Records 91 -- 100 Show 10 per page

Use the checkboxes to select records for output. See the sidebar for options.

- 91. **BRANDON DG, PERRY AJ**
[COMPUTER ANALYSIS OF DISLOCATED SPHERICAL CRYSTAL SURFACES](#)
PHILOSOPHICAL MAGAZINE 16 (139): 131& 1967
Times Cited: [19](#)

- 92. **BRANDON DG**
[STRUCTURE OF HIGH-ANGLE GRAIN BOUNDARIES](#)
ACTA METALLURGICA 14 (11): 1479& 1966
Times Cited: [714](#)

- 93. **BRANDON DG**
[IMAGE CONVERSION IN FIELD-ION MICROSCOPY](#)
JOURNAL OF SCIENTIFIC INSTRUMENTS 43 (10): 708& 1966
Times Cited: [4](#)

- 94. **BRANDON DG**
[ON FIELD EVAPORATION](#)
PHILOSOPHICAL MAGAZINE 14 (130): 803& 1966
Times Cited: [50](#)


Brandon Criterion, contd.

- Thus, if:

$$\theta_m < \nu_0 \Sigma_m^{-1/2} < 15^\circ m^{-1/2}$$

then we accept the boundary as belonging to the CSL of type $\Sigma=m$.

- The justification is based on the existence of a dislocation structure for vicinal interfaces to CSL structures, just as for low angle boundaries [see fig. 2.33 from Sutton & Balluffi]. Typical cutoff at $\Sigma=29$.

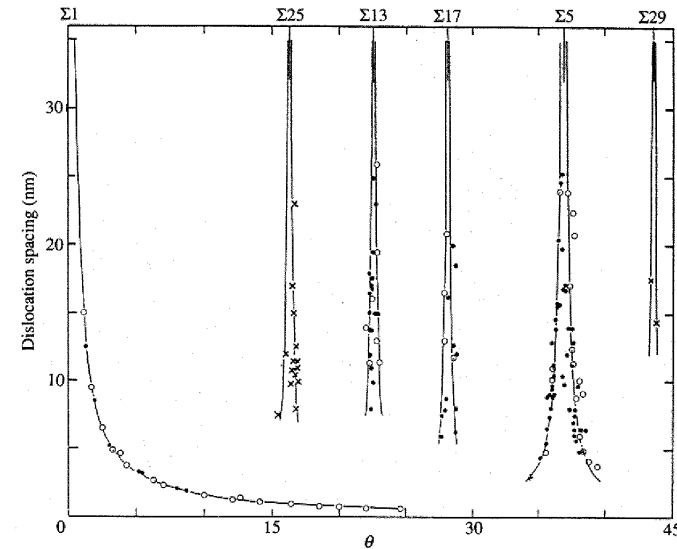


Fig. 2.33 Observed dislocation spacings in manufactured (001) twist grain boundaries in gold as a function of the twist angle. The lines show the spacings expected by Frank's formula, eqn (2.193), for DSC dislocations of the $\Sigma 1$, 5, 13, 17, 25, and 29 orientations. (From Babcock and Balluffi (1987).)

How near to a CSL?

- A reasonable way to measure distance from a special boundary type and an arbitrarily specified boundary is to calculate a minimum rotation angle (“orientation distance”) in exactly the same way as for the disorientation. In terms of Rodrigues vectors, we write the following for the composition of two rotations, $\rho_1\rho_2$, which represents ρ_1 followed by ρ_2 :

Composition of Rodrigues vectors

$$\rho_1 \bullet \rho_2 = \frac{\rho_1 + \rho_2 - \rho_1 \times \rho_2}{1 - \rho_1 \cdot \rho_2}$$

- To use this, we simply assign the components of a CSL boundary type to one of the Rodrigues vectors (strictly speaking, the inverse rotation, although the negative rotation is always equivalent to the positive one).

$$\rho_{g.b.} \bullet (-\rho_{CSL}) = \frac{\rho_{g.b.} - \rho_{CSL} + (\rho_{g.b.} \times \rho_{CSL})}{1 + (\rho_{g.b.} \cdot \rho_{CSL})}$$

- As always, one must use the crystal symmetry operators in order to find the smallest available angle. **Unless both the CSL value and the misorientation have been placed in the fundamental zone, then one will obtain the wrong result.**

Angle from CSL

One can then extract the angle, θ , from the length of the resultant vector (Chapter 3), where ρ is the Rodrigues vector description of the boundary in question and $|\rho|$ is the rotation angle associated with the vector:

$$\theta_0 = |\rho \cdot \rho_{000/0^\circ}| = |\rho \cdot \rho_{\Sigma 1}|, \rho_{\Sigma 1} = (0, 0, 0)$$

$$\theta_1 = |\rho \cdot \rho_{111/60^\circ}| = |\rho \cdot \rho_{\Sigma 3}|, \rho_{\Sigma 3} = (1/3, 1/3, 1/3)$$

$$\theta_3 = |\rho \cdot \rho_{111/38.21^\circ}|, \rho_{\Sigma 7} = (0.2, 0.2, 0.2)$$

Deviation from a CSL

- The deviation of a given misorientation from an exact misorientation type, such as a CSL type, is found by forming the product of the misorientation to be tested, and the inverse of the reference type.
- Given a $\Delta g = (O_B g_B)(O_A g_A)^{-1}$, and a reference type, Δg_{CSL} , then form the product

$$\Delta g' = \Delta g (\Delta g_{CSL})^{-1}.$$
- As stated before, it is necessary to apply *all* the relevant (crystal) symmetry operators (including the switching symmetry) to the Δg in order to ensure that the variant that is closest to the reference type is included in the comparison. This means that the result must be chosen that produces the minimum angle *and* that places the misorientation axis in the fundamental zone.
- Given the product “mis-misorientation”, one usually only considers the magnitude (rotation angle) extracted from it.
- All these operations can be performed with matrices, Rodrigues vectors, or (unit) quaternions. Most serious software uses quaternions.

Algorithm for Disorientation: 1

- To find the disorientation*, as just an angle, associated with a grain boundary but not identifying which symmetry operator was required for each crystal:
 1. Make a list of all crystal symmetry operators;
 2. Loop over switching symmetry (2 passes), which computes both Δg_{AB} and Δg_{BA} ;
 3. Loop over O_A (24 different operators, for cubic xtal symmetry);
 4. Calculate $\Delta g = g_B (O_A g_A)^{-1}$ or $(O_A g_A) g_B^{-1}$ and extract the angle (e.g. as arc-cosine of $[\text{trace}(\Delta g) - 1]/2$), depending on the first loop;
 5. If (misorientation) angle is lower than the previous result then retain the result (as the current candidate for the disorientation);
 6. End of loops: the misorientation that satisfied the tests is the disorientation because it possesses the minimum rotation angle. The misorientation axis can be placed in a single standard stereographic triangle by making all the indices positive that are associated with the minimum angle, and re-ordering so as to make $h \leq k \leq l$, for example.

*Disorientation:= combination of minimum angle and axis located in the fundamental zone

Algorithm for Disorientation: 2

- To find the disorientation* associated with a grain boundary and identify which symmetry operator on each crystal provided the disorientation (useful for analyzing 5-parameter grain boundary character):
 1. List all relevant symmetry operators;
 2. Compute both $\Delta_{g_{AB}}$ and $\Delta_{g_{BA}}$ (for switching symmetry); first loop over switching symmetry (2 passes);
 3. Second loop over O_A ;
 4. Third loop over O_B to calculate $\Delta g = (O_B g_B)(g_A O_A)^{-1}$ or $(O_A g_A)(g_B O_B)^{-1}$, depending on the first loop;
 5. If (misorientation) rotation axis associated with Δg lies within the fundamental zone (e.g. 100-110-111 SST for cubic), then proceed to the next test (treat the first such finding as a special case, i.e. retain the result and do *not* apply the next test);
 6. If (misorientation) angle is lower than the previous result then retain the result (as the current candidate for the disorientation);
 7. End of loops: the misorientation that satisfied the tests is the disorientation because it lies within the fundamental zone and possesses the minimum rotation angle.
 8. For any subsequent calculations, e.g. of boundary normal, ensure that you use the same symmetry operator in each grain as was found to yield the disorientation.

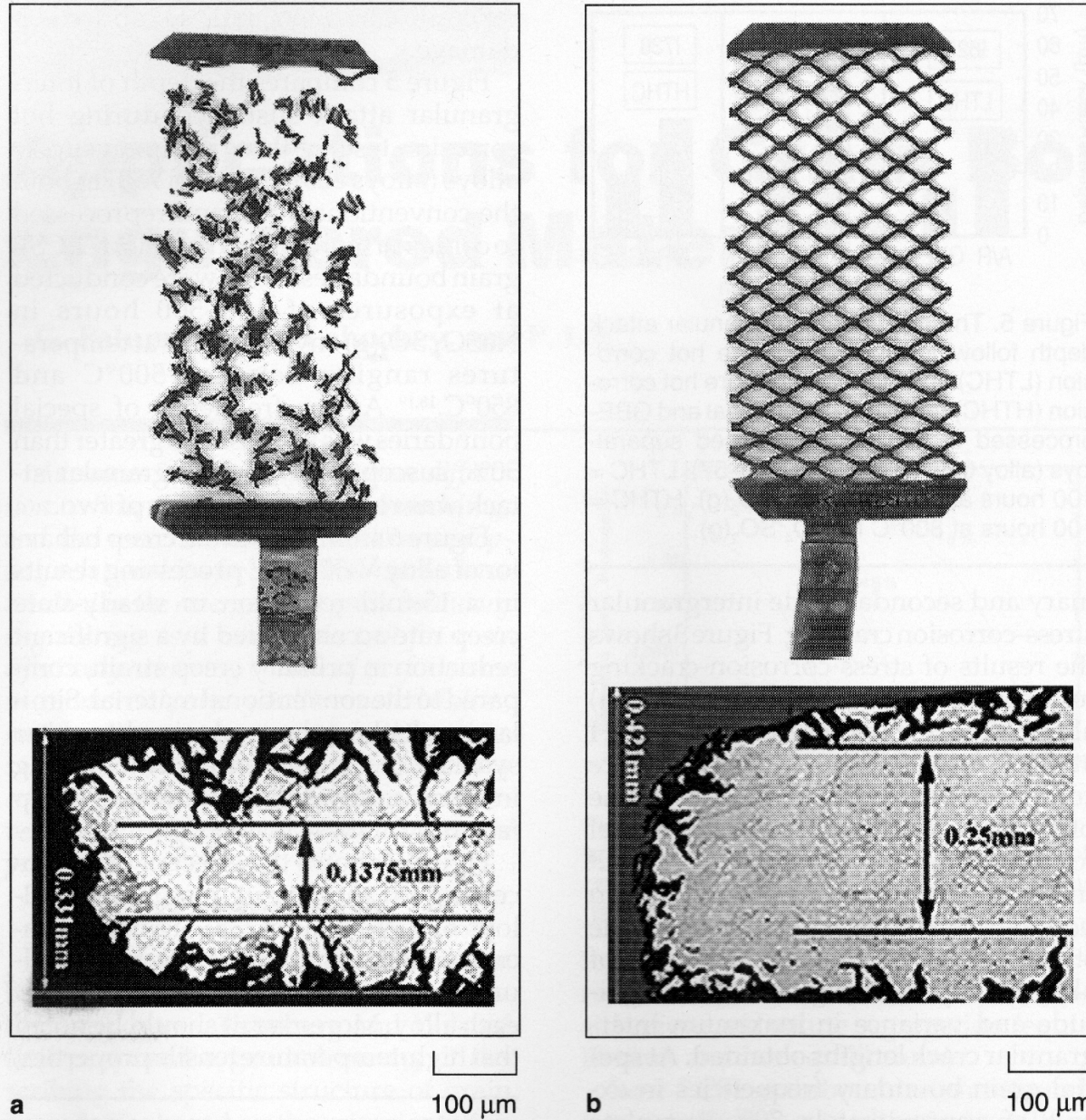
*Disorientation:= combination of minimum angle and axis located in the fundamental zone

Example: Effect of GB CD on Pb Electrodes in Lead-Acid Batteries

Palumbo et al. [Palumbo, G., E. M. Lehockey, and P. Lin (1998). "Applications for grain boundary engineered materials." JOM 50(2): 40-43.] have shown that the crystallographic nature of grain boundaries in Pb have a strong effect on the resistance of Pb electrodes (in the form of lattice-work grids) to failure via intergranular corrosion and creep-cracking. More specifically, Pb that has been processed to have a high fraction of special boundaries, i.e. coincidence site lattice boundaries with low sigma numbers, exhibit significantly longer lifetimes.

Pb electrodes, contd.

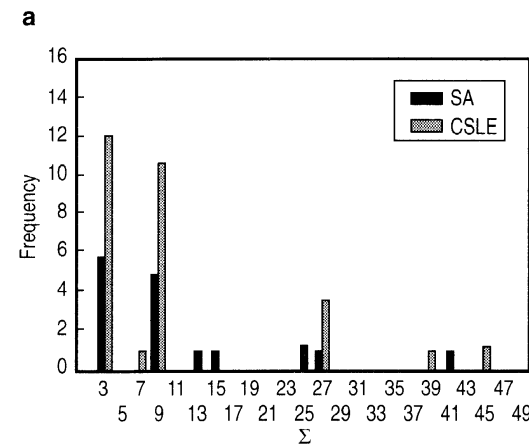
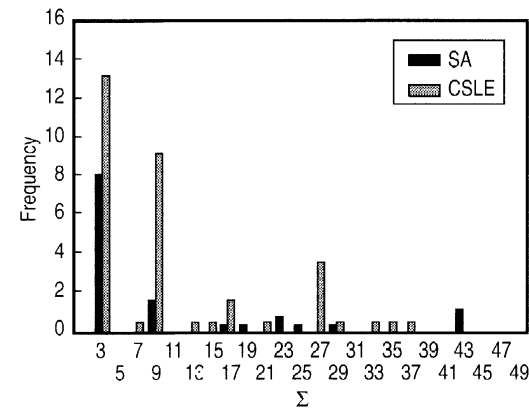
The figure (next slide) illustrates the difference in performance for Pb-Ca-Sn-Ag lead-acid positive battery grids following 40 charge-discharge cycles. The image on the left is the as-cast material with 7% special boundaries ($3 \leq \Sigma \leq 29$); the image on the right is the grain boundary engineered material with 67.6% special boundaries. The small amount of Ca added to Pb is a hardening agent (from the eutectic at 0.07% Ca).



a **b**
100 μm 100 μm
Figure 8. The condition of (a) conventional and (b) GBE-processed Pb-Ca-Sn-Ag lead-acid positive battery grids following 40 charge-discharge cycles (1–1.781 V direct current) in H_2SO_4 at 70°C.

Example: creep resistance in Inconel 600: Ni-16Cr-9Fe

- Creep resistance of Ni-alloys is strongly enhanced by maximizing the fraction of special boundaries.
- Solution annealed (SA) vs. CSL-enhanced (CSLE): note higher frequencies of low- Σ boundaries.



b
Figure 1. An example of the grain boundary character distribution in (a) coarse grain (330 μm) and (b) small grain (35 μm) SA and CSLE samples.

Was, G. S., V. Thavepringsriporn, et al. (1998). "Grain boundary misorientation effects on creep and cracking in Ni-based alloys." *JOM* 50(2): 44-49.

Creep Resistance

Standard Material

*Grain
Boundary
Engineered*

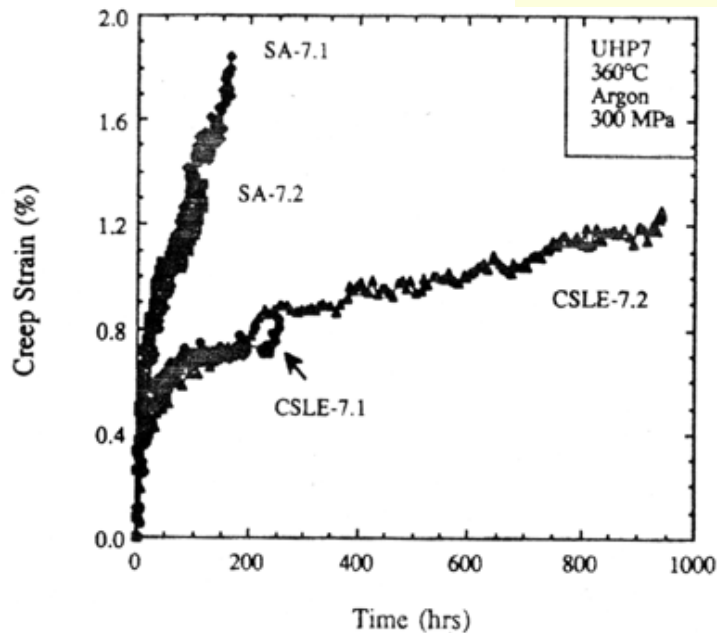


Fig. 2—Constant load creep curves of the coarse-grain SA and CSLE samples in 360 °C argon at 300 MPa.

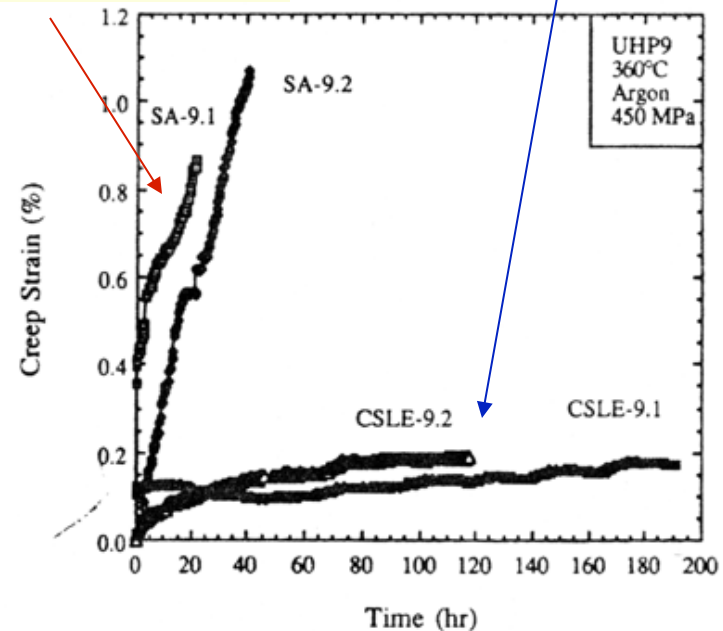


Fig. 3—Creep behavior of small-grain SA and CSLE samples at an initial stress of 450 MPa in 360 °C argon.

- Constant load creep curves show dramatic improvement in creep resistance from samples with normal boundaries, and [grain boundary engineered] GBE samples with a high fraction of CSL boundaries.

Creep Rates

- Creep resistance thought to be enhanced by resistance of CSL boundaries to recovery of extrinsic dislocations. Lack of recovery in CSLs means higher back stresses opposing creep stress, therefore lower strain rate.

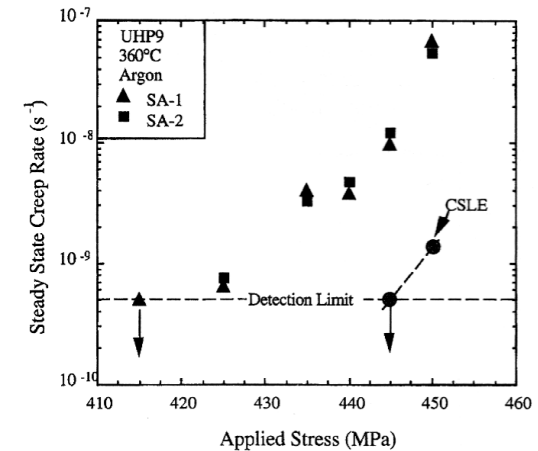


Figure 3. The dependence of the steady-state creep rate on applied stress for two small-grain SA samples and a CSLE sample in 360°C argon.

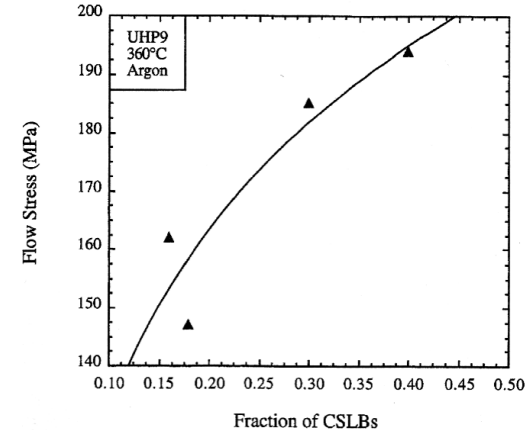


Figure 4. The dependence of flow stress on CSLB fraction after straining at a constant extension rate to 1.25% plastic strain in 360°C argon.

Mechanism

Dislocations (extrinsic grain boundary dislocations) accumulate in CSL boundaries giving rise to back stresses that oppose creep.

V. Thaveepriingsriporn and Was, G. S. (1997). "The role of CSL boundaries in creep of Ni-16Cr-9Fe at 360°C." *Metall. Trans.* **28A**: 2101.

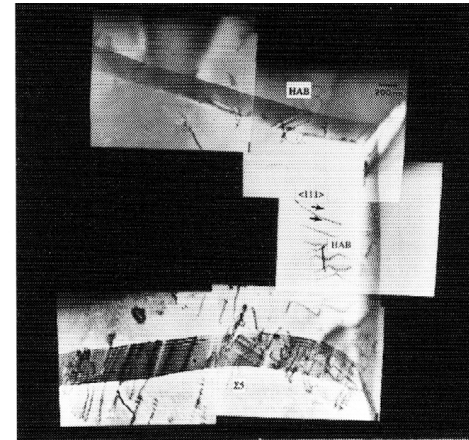


Figure 8. An example of EGBD density in random high-angle and CSL boundaries in an SA sample after 1.25% plastic strain in 360°C argon at a strain rate of $8 \times 10^{-7} \text{ s}^{-1}$.

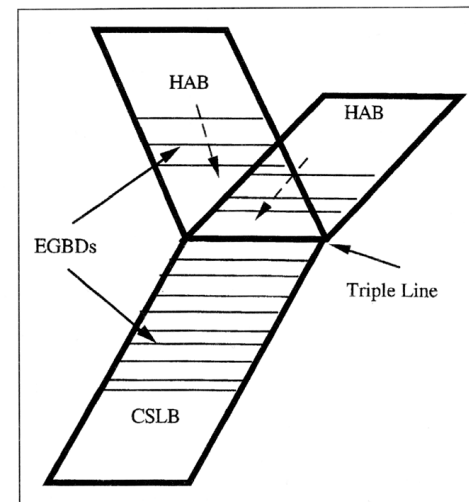


Figure 9. A schematic of dislocation annihilation at a triple line.

Creep of Ni: model

- The creep rate as a function of grain size and boundary type was modeled (after Sangal & Tangri) assuming that dislocation annihilation is much slower in CSL boundaries than in general boundaries.

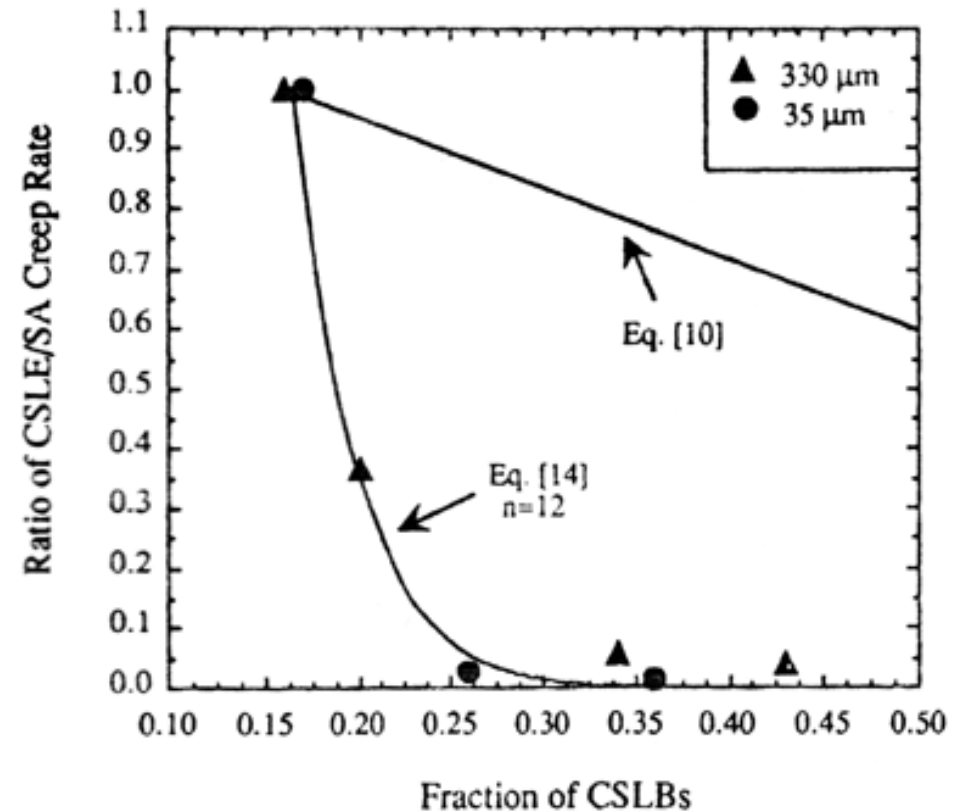


Fig. 11—Comparison of measured and calculated ratios (Eq. [14]) of CSLE/SA creep rate with the CSLB fraction in 330 and 35 μm grains crept at 300 and 450 MPa, respectively. Annihilation of EGBDs assumed to occur at the triple lines.

Grain Boundary Cracking

Cracking at grain boundaries in corrosion testing post-creep shows strong sensitivity to boundary type: CSL boundaries are less prone to corrosion attack.

V. Thaveeringsripor and Was, G. S. (1997). "The role of CSL boundaries in creep of Ni-16Cr-9Fe at 360°C." *Metall. Trans.* **28A**: 2101.

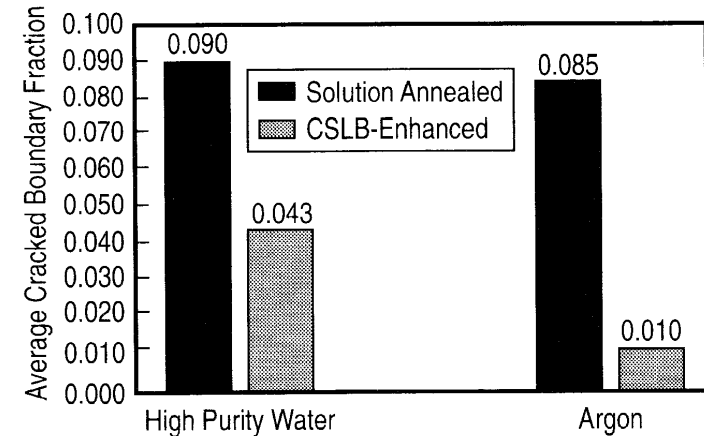


Figure 6. An average cracked boundary fraction for coarse-grain SA and CSLE samples after constant extension rate tests in 360°C high-purity water or argon.

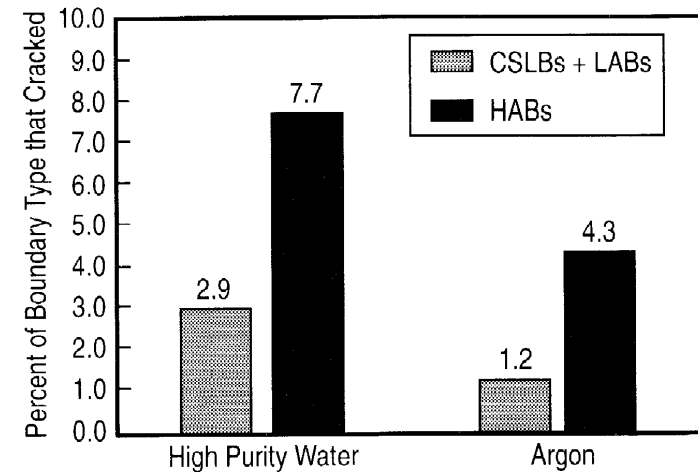


Figure 7. The percentage of total boundary types that cracked (coarse-grain SA and CSLE samples combined) after constant extension rate tests at 360°C in high-purity water or argon.

Grain Boundary Properties

- Based on these remarks on grain boundary structure, one might expect that CSL boundaries (especially in the pure twist or tilt boundary alignment) would have low energy because of good atomic fit.
- Some observations support this, e.g. deposition of small particles on a single crystal shows that low-sigma CSL boundaries are favored.
- “Grain boundary engineering” relies on simply maximizing the (area) fraction of CSL boundaries. This is typically made quantitative by adopting Brandon’s criterion and counting the fraction of boundaries that are associated with $\Sigma \leq 29$.
- Observations of grain boundary character MgO [Saylor & Rohrer] suggest otherwise: the low surface energy plane tends to dominate the grain boundary distribution, and is associated with low boundary energy in all crystalline materials.
- It turns out that fcc metals are the exception because of their exceptionally low coherent twin boundary energy, which, in Ni & Cu (for example) is about 5% of the high angle GB energy. This promotes the formation of annealing twins, which in turn result in related CSL types being present such as $\Sigma 9$, $\Sigma 27$.

Summary

- The *Coincident Site Lattice* is a useful concept for identifying boundaries with low misfit (thus, low energy) in fcc metals.
- *Brandon's criterion*: Standard analysis of orientation distance leads to a criterion for how close a given grain boundary is to a particular CSL type. Brandon's criterion provides a numerical measure that is based on the concept of interfacial dislocations that accommodate small departures from an exact CSL relationship.
- *Grain Boundary Engineering* relies upon CSL analysis.
- *Macroscopic Degrees of Freedom*: In general, five parameters needed to describe crystallographic grain boundary character. This is apparent in the combination of CSL misorientation relationship and twist or tilt boundary plane (to maximize CSL point density in the boundary plane).
- *Caution*: the CSL theory applies to lattice sites, not atom positions. Evidence suggests strongly that in all except fcc metals, the properties are related to the two surfaces that make up the boundary, not the CSL structure. The existence of low energy boundaries for e.g., $\Sigma 3$ and $\Sigma 11$ boundaries is "coincidence".

Supplemental Slides

- Information on CSL relationships in hcp metals, courtesy of Nathalie Bozzolo, CEMEF, France.

CSL list for HCP

Axis (cart ^(*) /hex)	Angle (°)	Σ	close to Twin Axis, angle, plane	Ti 3 μ m	Zr 5.5 μ m	Zr 17.0 μ m
001 / 0001	13.2	19a		X	X	X
001 / 0001	21.8	7a		X	X	X
001 / 0001	27.8	13a		X	X	X
100 / 10-10	35.1	11a	[1-100] 34.85° (11-21)	X	X	X
100 / 10-10	55.6	23a		No	No	No
100 / 10-10	64.6	7b	[1-100] 64.23° (11-22)	X	X	X
100 / 10-10	76.7	13c		X	X	No
100 / 10-10	87.0	19c		X	X	X
010 / 2-1-10	40.1	17a		No	X	X
010 / 2-1-10	57.4	13b		X	X	X+
010 / 2-1-10	72.3	23b		No	X	X
010 / 2-1-10	84.8	11b	[11-20] 84.79° (1-102)	X	X	X
/ 3-1-20	79.8	17b		No	No	No
/10,0,-10,3	86.3	23c		No	No	No
/10,-5,-5,3	65.1	19b		X	X	X+
(*) Y-convention						

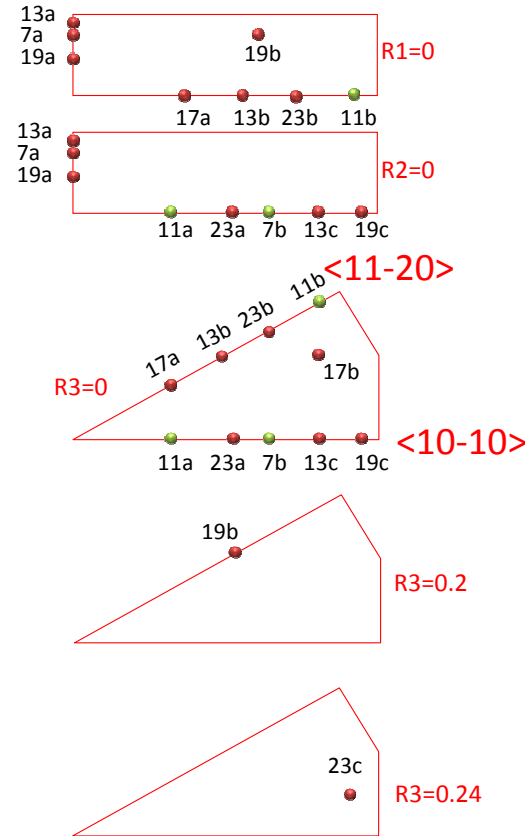
R. Bonnet, E. Cousineau, D.H. Warrington "Determination of near-coincident cells for hexagonal crystals. Related DSC lattices" Acta Crystallographica, A37 (1981) 184-189

Bozzolo *et al.* (2010). "Misorientations induced by deformation twinning in titanium." J. Appl. Crystallography **43** 596-602

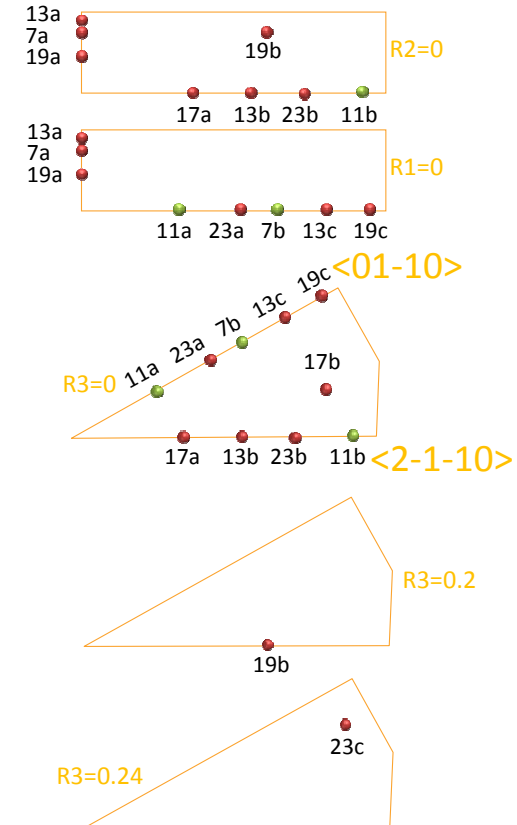
CSLs for HCP in RF space

- Note the two different conventions for alignment of the orthonormal coordinate system (used for calculations) with the crystallographic axes. Typically Channel (HKL) systems use the Y-convention whereas EDAX (TSL/OIM) systems use the X-convention.
- Certain CSL relationships correspond to deformation twins observed in Ti and Zr.

CSLs located in RF space within X or Y convention :



$r_1 = \langle 01-10 \rangle$ ("Y-convention")



$r_1 = \langle 2-1-10 \rangle$ ("X-convention")

- CSL
- CSL/Twin